Available online at www.sciencedirect.com
ScienceDirect
Ann. I. H. Poincaré – AN 25 (2008) 77–103
ANNALES DE L'INSTITUT HENRI POINCARÉ
ANALYSE NON LINÉAIRE
www.elsevier.com/locate/anihpc

Energies of S^2-valued harmonic maps on polyhedra with tangent boundary conditions

A. Majumdar [a,b], J.M. Robbins [a,*], M. Zyskin [a]

[a] *School of Mathematics, University of Bristol, University Walk, Bristol BS8 1TW, UK*
[b] *Hewlett-Packard Laboratories, Filton Road, Stoke Gifford, Bristol BS12 6QZ, UK*

Received 17 May 2006; accepted 13 November 2006

Available online 28 December 2006

Abstract

A unit-vector field $\mathbf{n}: P \to S^2$ on a convex polyhedron $P \subset \mathbb{R}^3$ satisfies tangent boundary conditions if, on each face of P, $\mathbf{n}$ takes values tangent to that face. Tangent unit-vector fields are necessarily discontinuous at the vertices of P. We consider fields which are continuous elsewhere. We derive a lower bound $E_P^-(h)$ for the infimum Dirichlet energy $E_P^{\inf}(h)$ for such tangent unit-vector fields of arbitrary homotopy type h. $E_P^-(h)$ is expressed as a weighted sum of minimal connections, one for each sector of a natural partition of S^2 induced by P. For P a rectangular prism, we derive an upper bound for $E_P^{\inf}(h)$ whose ratio to the lower bound may be bounded independently of h. The problem is motivated by models of nematic liquid crystals in polyhedral geometries. Our results improve and extend several previous results.

MSC: 35A15; 35A20; 35J50; 35J65; 55P15; 58E20; 82D30

Keywords: Harmonic maps with defects; Tangent boundary conditions; Minimal connection; Liquid crystals; Bistability

1. Introduction

S^2-valued harmonic maps on three-dimensional domains with holes were studied in a well known paper by Brezis, Coron and Lieb [4]. As a simple representative example, consider the domain $\Omega = \mathbb{R}^3 - \{\mathbf{r}^1, \dots, \mathbf{r}^n\}$ (for which the holes are points), and let $\mathbf{n}: \Omega \to S^2$ denote a unit-vector field on Ω. For $\nabla\mathbf{n}$ square-integrable, we define the Dirichlet energy of $\mathbf{n}$ to be

$$E(\mathbf{n}) = \int_{\Omega} (\nabla\mathbf{n})^2 \, \mathrm{d}V. \tag{1.1}$$

* Corresponding author.
E-mail addresses: a.majumdar@bristol.ac.uk (A. Majumdar), j.robbins@bristol.ac.uk (J.M. Robbins), m.zyskin@bristol.ac.uk (M. Zyskin).

0294-1449/$ – see front matter
doi:10.1016/j.anihpc.2006.11.003

Continuous unit-vector fields on Ω may be classified up to homotopy by their degrees, $d = (d^1, \dots, d^n) \in \mathbb{Z}^n$, on spheres about each of the excluded points (the restriction of $\mathbf{n}$ to such a sphere may be regarded as a map from S^2 into itself). In order that $\mathbf{n}$ have finite energy, we must have that

$$\sum_j d^j = 0. \tag{1.2}$$

Let $\mathcal{C}_\Omega(d)$ denote the homotopy class of continuous unit-vector fields with degrees d satisfying (1.2), and let $\mathcal{H}C_\Omega(d)$ denote the elements of $\mathcal{C}_\Omega(d)$ with finite Dirichlet energy. Let $E_\Omega^{\inf}(d)$ denote the infimum of the energy over $\mathcal{H}C_\Omega(d)$,

$$E_\Omega^{\inf}(d) = \inf_{\mathbf{n}\in\mathcal{H}C_\Omega(d)} E(\mathbf{n}). \tag{1.3}$$

It turns out that $E_\Omega^{\inf}(d)$ is just 8π times the length of a *minimal connection* on Ω. We recall the definition of a minimal connection. Given two m-tuples of points in $\mathbb{R}^3$, $\mathcal{P} = (\mathbf{a}^1, \dots, \mathbf{a}^m)$ and $\mathcal{N} = (\mathbf{b}^1, \dots, \mathbf{b}^m)$ (whose points need not be distinct), a connection is a pairing $(\mathbf{a}^j, \mathbf{b}^{\pi(j)})$ of points in $\mathcal{P}$ and $\mathcal{N}$, specified here in terms of a permutation $\pi \in S_m$ (S_m denotes the symmetric group). The length of a connection is the sum of the distances between the paired points, and a minimal connection is a connection with minimum length. Let

$$L(\mathcal{P}, \mathcal{N}) = \min_{\pi\in S_m} \sum_{j=1}^m \left|\mathbf{a}^j - \mathbf{b}^{\pi(j)}\right| \tag{1.4}$$

denote the length of a minimal connection between $\mathcal{P}$ and $\mathcal{N}$. Let $|d| = \frac{1}{2}\sum_j |d^j|$. Then

Theorem 1.1. [4] *The infimum $E_\Omega^{\inf}(d)$ of the Dirichlet energy of continuous unit-vector fields on the domain $\Omega = \mathbb{R}^3 - \{\mathbf{r}^1, \dots, \mathbf{r}^n\}$ of given degrees d^j about the excluded points $\mathbf{r}^j$ is given by*

$$E_\Omega^{\inf}(d) = 8\pi L\big(\mathcal{P}(d), \mathcal{N}(d)\big), \tag{1.5}$$

where $\mathcal{P}(d)$ is the $|d|$-tuple of excluded points of positive degree, with $\mathbf{r}^j$ included d^j times, and $N(d)$ is the $|d|$-tuple of excluded points of negative degree, with $\mathbf{r}^k$ included $|d^k|$ times.

In this paper we consider a natural variant of this problem which emerges from a boundary-value problem of some physical and technological interest; the domain is taken to be a polyhedron on which $\mathbf{n}$ is required to satisfy *tangent boundary conditions*. Let P denote a convex bounded polyhedron in $\mathbb{R}^3$, including the interior of the polyhedron but excluding its vertices. Let $\mathbf{n}: P \to S^2$ denote a unit-vector field on P. We say that $\mathbf{n}$ satisfies tangent boundary conditions, or is tangent, if, on each face of P, $\mathbf{n}$ takes values tangent to that face. (It is clear that this condition could not be satisfied at the vertices of the polyhedron, which belong to three or more faces.)

One motivation for the problem comes from liquid crystals applications, in which $\mathbf{n}$ describes the mean local orientation of a nematic liquid crystal, and the Dirichlet energy (1.6) coincides with the elastic or Frank–Oseen energy in the so-called one-constant approximation (see, e.g., [6,26,14,25]). Polyhedral cells have been proposed as a mechanism for engendering bistability – they may support two nematic configurations with distinct optical properties, both of which are local minima of the elastic energy [11,23,12,7,5,21]. In many cases of interest the orientation at interfaces is well described by tangent boundary conditions, and low-energy local minimisers appear to have different topologies. We also remark that harmonic maps between Riemannian polyhedra have been studied by Gromov and Shoen [9] and Eells and Flugede [8], in particular in cases where the target manifold has nonpositive curvature.

Here we will restrict our attention to continuous tangent unit-vector fields on P. (Let us note that, while nematic orientation is, in general, described by a director, or RP^2-valued field, a continuous director field on a simply connected domain such as P can be lifted to a continuous unit-vector field.) Continuous tangent unit-vector fields on P can be partitioned into homotopy classes $\mathcal{C}_P(h)$ labelled by a complete set of homotopy invariants denoted collectively by h. A full account of this classification is given in [24] (see also [28]). Below we reprise the results we need here. General discussions of topological defects in liquid crystals are given in [22,13,14].

For $\nabla\mathbf{n}$ square integrable on P, let

$$E(\mathbf{n}) = \int_P (\nabla\mathbf{n})^2 \, \mathrm{d}V \tag{1.6}$$

denote its Dirichlet energy. Let $\mathcal{H}C_P(h)$ denote the elements of $\mathcal{C}_P(h)$ with finite Dirichlet energy, and let

$$E_P^{\inf}(h) = \inf_{\mathbf{n}\in\mathcal{H}C_P(h)} E(\mathbf{n}) \tag{1.7}$$

denote the infimum of the energy over $\mathcal{H}C_P(h)$. Our first result (Theorem 1.2 below) is a lower bound for $E_P^{\inf}(h)$. This is expressed in terms of certain homotopy invariants called wrapping numbers, which we now define. Let f denote the number of faces of P, F^c the cth face of P, and $\mathbf{F}^c$ the outward normal on F^c, where $1 \leqslant c \leqslant f$. For each face we consider the great circle on S^2 containing the unit-vectors $\mathbf{s}$ tangent to it, i.e. $\mathbf{F}^c \cdot \mathbf{s} = 0$. These f (not necessarily distinct) great circles partition S^2 into open spherical polygons, which we call *sectors*. The sectors are characterised by $\operatorname{sgn}(\mathbf{F}^c \cdot \mathbf{s})$. We write

$$S^\sigma = \{\mathbf{s} \in S^2 \mid \operatorname{sgn}(\mathbf{s}\cdot\mathbf{F}^c) = \sigma^c\}, \tag{1.8}$$

where $\sigma = (\sigma^1, \ldots, \sigma^f)$ is an f-tuple of signs. It should be noted that most of the S^σ's are empty; indeed, reckoning based on Euler's formula for polygonal partitions of the sphere (|vertices| − |edges| + |faces| = 2) shows that there are at most (and generically) $f^2 - f + 2$ nonempty sectors.

Next, let C^a denote a smooth surface in P which separates the vertex $\mathbf{v}^a$ from the others. For definiteness, take C^a to be oriented so that $\mathbf{v}^a$ lies on the positive side of C^a. We call C^a a *cleaved surface*. Given $\mathbf{n} \in \mathcal{C}_P(h)$, let $\mathbf{n}^a$ denote its restriction to C^a. The wrapping number $w^{a\sigma}$ is the number of times $\mathbf{n}^a$ covers S^σ, counted with orientation. For $\mathbf{n}$ differentiable, this is given by

$$w^{a\sigma} = \frac{1}{A^\sigma} \int_{C^a} \mathbf{n}^*(\chi^\sigma \omega), \tag{1.9}$$

where ω is the area two-form on S^2, normalised to have integral 4π, χ^σ is the characteristic function of $S^\sigma \subset S^2$, and $A^\sigma = |\int_{S^2} \chi^\sigma \omega|$ is the area of S^σ. Alternatively, $w^{a\sigma}$ can be expressed as the index of a regular value $\mathbf{s} \in S^\sigma$ of $\mathbf{n}^a$, i.e.

$$w^{a\sigma} = \sum_{\mathbf{r}|\mathbf{n}^a(\mathbf{r})=\mathbf{s}} \operatorname{sgn}\det d\mathbf{n}^a(\mathbf{r}). \tag{1.10}$$

One can show that $w^{a\sigma}$ does not depend on the choice of $\mathbf{s} \in S^\sigma$ nor on the choice of cleaving surface C^a, that the definition (1.9) can be extended to continuous $\mathbf{n}$, and that its value depends only on the homotopy class of $\mathbf{n}$ [24]. In fact, the wrapping numbers constitute a complete set of invariants, as is shown in Appendix A. They are not independent, however. For example, continuity in the interior of P (absence of singularities) implies that, for all σ,

$$\sum_a w^{a\sigma} = 0, \tag{1.11}$$

where the sum is taken over vertices $\mathbf{v}^a$. Continuity on the faces and edges of P implies additional constraints. We will say that $h = \{w^{a\sigma}\}$ is an *admissible topology* if it can be realised by some continuous configuration $\mathbf{n}: P \to S^2$.

Theorem 1.2. *Let $h = \{w^{a\sigma}\}$ be an admissible topology for continuous tangent unit-vector fields on a polyhedron P. Then*

$$E_P^{\inf}(h) \geqslant E_P^-(h) := \sum_\sigma 2A^\sigma L(\mathcal{P}^\sigma(h), \mathcal{N}^\sigma(h)), \tag{1.12}$$

where $\mathcal{P}^\sigma$ (resp. $\mathcal{N}^\sigma$) contains the vertices of P for which $w^{a\sigma}$ is positive (resp. negative), each such vertex included with multiplicity $|w^{a\sigma}|$.

Thus, to each sector σ may be associated a constellation of point defects at the vertices $\mathbf{v}^a$ of degrees $w^{a\sigma}$. The lower bound $E_P^-(h)$ is a sum of the lengths of minimal connections for these constellations weighted by the areas of the sectors.

Theorem 1.2 is proved using arguments similar to those used to show that $E_\Omega^{\inf}(d) \geqslant 8\pi L(\mathcal{P}(d), \mathcal{N}(d))$ in the proof of Theorem 1.1. In Theorem 1.1, one obtains an equality for $E_\Omega^{\inf}(d)$, rather than just a lower bound, by constructing a sequence $\mathbf{n}^{(j)}$ whose energies approach $8\pi L(\mathcal{P}(d), \mathcal{N}(d))$. It can be shown that a subsequence $\mathbf{n}^{(k)}$ approaches a constant away from a minimal connection while $|\nabla \mathbf{n}^{(k)}|^2$ approaches a singular measure supported on the minimal connection [4]. In the present case, tangent boundary conditions preclude such a construction; $\mathbf{n}$ is required to vary across the faces and, therefore, throughout the interior of P. However, for P a rectangular prism, we can show that $E_P^-(h)$ correctly describes the dependence of the infimum energy on homotopy type.

Theorem 1.3. *Let P denote a rectangular prism with sides of length $L_x \geqslant L_y \geqslant L_z$ and largest aspect ratio $\kappa = L_x/L_z$. Then*

$$E_P^{\inf}(h) \leqslant C\kappa^3 E_P^-(h) \tag{1.13}$$

for some constant C independent of h and L_x, L_y, L_z.

The upper bound of Theorem 1.3 is obtained by estimating the energy of explicitly constructed tangent unit-vector fields which satisfy the Euler–Lagrange equations near each vertex.

The general form of the Frank–Oseen energy is given by [6,26,14,25]

$$E_{\mathrm{FO}}(\mathbf{n}) = \int_P \left[K_1(\operatorname{div}\mathbf{n})^2 + K_2(\mathbf{n}\cdot\mathbf{curl}\,\mathbf{n})^2 + K_3(\mathbf{n}\times\mathbf{curl}\,\mathbf{n})^2 + K_4 \operatorname{div}\big((\mathbf{n}\cdot\nabla)\mathbf{n} - (\operatorname{div}\mathbf{n})\mathbf{n}\big)\right] \mathrm{d}V, \tag{1.14}$$

where the elastic constants K_j are material-dependent. It is easily shown that tangent boundary conditions imply that the contribution from the K_4-term in (1.14) vanishes. The elastic constants K_1, K_2 and K_3 are constrained to be nonnegative, and the one-constant approximation (1.6) follows from taking $K_1 = K_2 = K_3 = 1$. We remark that Theorems 1.2 and 1.3 imply the following bounds for the Frank–Oseen energy:

$$K_- E_P^-(h) \leqslant \inf_{\mathbf{n}\in\mathcal{HC}_P(h)} E_{\mathrm{FO}}(\mathbf{n}) \leqslant CK_+\kappa^3 E_P^-(h), \tag{1.15}$$

where K_- (resp. K_+) is the smallest (resp. largest) of the elastic constants K_1, K_2 and K_3.

Theorems 1.2 and 1.3 improve and extend several earlier results. In [19] we obtained a lower bound for $E_P^{\inf}(h)$ of the form

$$2\max_{\xi^a} \sum_a \xi^a \left(\sum_\sigma A^\sigma w^{a\sigma}\right), \tag{1.16}$$

where the maximum is taken over ξ^a's such that $|\xi^a - \xi^b| \leqslant |\mathbf{v}^a - \mathbf{v}^b|$. The quantity (1.16) is generally less than the lower bound given by Theorem 1.2, in particular because it allows for cancellations between wrapping numbers of opposite sign. For example, for a regular tetrahedron with sides of unit length, (1.16) gives a lower bound of $\sum_{a\sigma} A^\sigma w^{a\sigma}$, whereas Theorem 1.2 gives the lower bound $\sum_{a\sigma} A^\sigma |w^{a\sigma}|$. For a rectangular prism, Theorem 1.3 does not hold if (1.16) is substituted for $E_P^-(h)$. ((1.16) can be directly compared to (2.15) below, which gives an equivalent (dual) expression for $E_P^-(h)$.) A restricted example of Theorem 1.2 was given in [20] for the case h is a *reflection-symmetric topology*. These are the topologies of configurations which are invariant under reflections through the midplanes of the prism.

Results related to Theorem 1.3 were obtained for the special case of reflection-symmetric topologies in [18,20]. The constructions and estimates are simpler in this case, and one can show that the ratio of the upper and lower bounds scales linearly with the aspect ratio κ, rather than as κ^3. Indeed, for conformal and anticonformal reflection-symmetric topologies (for which the wrapping numbers $w^{a\sigma}$ about a given vertex have the same sign), one can show that the ratio is bounded by $(L_x^2 + L_y^2 + L_z^2)^{1/2}/L_z$. It is not clear that for general prism topologies the κ^3 dependence in Theorem 1.3 is optimal.

An important question is whether within a given homotopy class the infimum Dirichlet energy is achieved. The homotopy classes $\mathcal{HC}_P(h)$ are not weakly closed with respect to the Sobolev norm, so it is not automatically the case that the infimum is achieved. However, while a given $\mathcal{HC}_P(h)$ may not be weakly closed, it may still contain a local (smooth) minimiser of the Dirichlet energy. Indeed, there is some numerical evidence and heuristics to suggest that, in the case of a rectangular prism, for the simplest topologies a smooth minimiser always exists, while for others a smooth local minimiser may or may not exist depending on the aspect ratios [18,17]. It would be interesting to establish for which topologies there exist smooth local minimisers, also from the point of view of device applications. Such configurations would of course satisfy the bounds established here.

There is an extensive literature on S^2-valued harmonic maps with fixed (Dirichlet) boundary data; reviews are given in [10,3]. Problems related to the one considered here concern liquid crystal droplets [15,26], in which one seeks configurations $\mathbf{n}$ on a three-dimensional region Ω which minimise the elastic energy [16]. In case of tangent boundary conditions, there are necessarily singularities on the surface of Ω, e.g. 'boojums' [27]; in a polyhedral domain, these singularities are pinned at the vertices.

The remainder of the paper is organised as follows. Theorem 1.2 is proved in Section 2, and Theorem 1.3 in Section 3 modulo two lemmas concerning the explicit construction of and estimates for the representative prism configurations (Sections 4 and 5). In Appendix A it is shown that homotopy classes of continuous tangent unit-vector fields on P are classified by wrapping numbers.

2. Lower bound for general polyhedra

Proof of Theorem 1.2. In [19] we show that smooth $\mathbf{n}$'s are dense in $\mathcal{HC}_P(h)$ with respect to the Sobolev $W^{(1,2)}$-norm. Therefore, it suffices to establish the lower bound (1.12) for $\mathbf{n}$ smooth.

Let $B_\epsilon(\mathbf{v}^a)$ denote the ϵ-ball about $\mathbf{v}^a$, and let

$$P_\epsilon = P - \bigcup_a \big(B_\epsilon(\mathbf{v}^a) \cap P\big) \tag{2.1}$$

denote the domain obtained by excising these balls from P. Clearly

$$E(\mathbf{n}) = \int_P (\nabla \mathbf{n})^2 \, \mathrm{d}V \geqslant \int_{P_\epsilon} (\nabla \mathbf{n})^2 \, \mathrm{d}V. \tag{2.2}$$

Let χ^σ denote the characteristic function of the sector $S^\sigma \subset S^2$. It will be useful to introduce smooth approximations $\tilde{\chi}^\sigma$ to χ^σ, such that $\tilde{\chi}^\sigma$ has support in S^σ and satisfies $0 \leqslant \tilde{\chi}^\sigma \leqslant \chi^\sigma$. Then

$$E(\mathbf{n}) \geqslant \sum_\sigma \int_{P_\epsilon} \big(\tilde{\chi}^\sigma \circ \mathbf{n}\big)(\nabla \mathbf{n})^2 \, \mathrm{d}V. \tag{2.3}$$

Using the inequality [4]

$$(\nabla \mathbf{n})^2 \geqslant 2\|\mathbf{n}^*\omega\|, \tag{2.4}$$

where $\mathbf{n}^*\omega$ denotes the pullback of ω by $\mathbf{n}$ and $\|\cdot\|$ denotes the norm on forms induced by the standard metrics on $\mathbb{R}^3$ and S^2, we get that

$$E(\mathbf{n}) \geqslant 2\sum_\sigma \int_{P_\epsilon} \big\|\mathbf{n}^*\big(\tilde{\chi}^\sigma \omega\big)\big\| \, \mathrm{d}V. \tag{2.5}$$

For each σ, let ξ^σ denote a continuous piecewise-differentiable function on P with

$$\big\|\mathrm{d}\xi^\sigma\big\| \leqslant 1. \tag{2.6}$$

Then for arbitrary $\mathbf{a}$, $\mathbf{b}$, $\mathbf{c}$, we have that

$$\|\mathbf{n}^*\omega\| \big|\mathrm{d}V(\mathbf{a},\mathbf{b},\mathbf{c})\big| \geqslant \big(\mathrm{d}\xi^\sigma \wedge \mathbf{n}^*\omega\big)(\mathbf{a},\mathbf{b},\mathbf{c}), \tag{2.7}$$

where dV is here regarded as the Euclidean volume form on $\mathbb{R}^3$. But

$$\mathrm{d}\xi^\sigma \wedge \mathbf{n}^*\big(\tilde{\chi}^\sigma \omega\big) = \mathrm{d}\big(\xi^\sigma \mathbf{n}^*\big(\tilde{\chi}^\sigma \omega\big)\big), \tag{2.8}$$

since $\mathrm{d}(\mathbf{n}^*(\tilde{\chi}^\sigma \omega)) = \mathbf{n}^*\mathrm{d}(\tilde{\chi}^\sigma \omega) = 0$ ($\tilde{\chi}^\sigma \omega$ is a two-form on S^2). Therefore,

$$E(\mathbf{n}) \geqslant 2\sum_\sigma \int_{P_\epsilon} \mathrm{d}\big(\xi^\sigma \mathbf{n}^*\big(\tilde{\chi}^\sigma \omega\big)\big). \tag{2.9}$$

From Stokes' theorem, (2.9) implies that

$$E(\mathbf{n}) \geqslant 2\sum_\sigma \int_{\partial P_\epsilon} \xi^\sigma \mathbf{n}^*\big(\tilde{\chi}^\sigma \omega\big). \tag{2.10}$$

The boundary of P_ϵ consists of (i) the faces of P with points in $B_\epsilon(\mathbf{v}^a)$ removed, and (ii) the intersections of the two-spheres $\partial B_\epsilon(\mathbf{v}^a)$ with P. The latter, denoted by $C_\epsilon^a = \partial B_\epsilon(\mathbf{v}^a) \cap P$, we call *cleaved surfaces*. Tangent boundary conditions imply that $\mathbf{n}^*\omega$ vanishes on the faces of P (since the values of $\mathbf{n}$ on a face are restricted to a great circle in S^2). Therefore, only the cleaved surfaces contribute to the integral in (2.10). We obtain

$$E(\mathbf{n}) \geqslant 2\sum_\sigma \sum_a \int_{C_\epsilon^a} \xi^\sigma \mathbf{n}^*\big(\tilde{\chi}^\sigma \omega\big). \tag{2.11}$$

We can replace $\tilde{\chi}^\sigma$ by χ^σ in (2.11) (by the bounded convergence theorem). Taking the limit $\epsilon \to 0$, we obtain

$$E(\mathbf{n}) \geqslant 2\sum_\sigma \sum_a \xi^\sigma\big(\mathbf{v}^a\big) \lim_{\epsilon\to 0} \int_{C_\epsilon^a} \mathbf{n}^*\big(\chi^\sigma \omega\big). \tag{2.12}$$

From (1.9), the integral over C_ϵ^a yields A^σ times the wrapping number $w^{a\sigma}$, which depends only on the homotopy type of $\mathbf{n}$. Thus,

$$E_P^{\inf}(h) \geqslant 2\sum_\sigma A^\sigma \sum_a \xi^\sigma\big(\mathbf{v}^a\big) w^{a\sigma}. \tag{2.13}$$

The remainder of the argument proceeds as in [4]. We note that (2.13) holds for any choice of ξ^σ's consistent with the constraints (2.6). These constraints imply that

$$\big|\xi^\sigma\big(\mathbf{v}^a\big) - \xi^\sigma\big(\mathbf{v}^b\big)\big| \leqslant \big|\mathbf{v}^a - \mathbf{v}^b\big|. \tag{2.14}$$

Conversely, given any set of values $\xi^{a\sigma}$ for which $|\xi^{a\sigma} - \xi^{b\sigma}| \leqslant |\mathbf{v}^a - \mathbf{v}^b|$, we can find functions ξ^σ which satisfy the constraints (2.6) and assume these values at the vertices (for example, take $\xi^\sigma(\mathbf{r}) = \max_a(\xi^{a\sigma} - |\mathbf{r} - \mathbf{v}^a|)$). Thus, we obtain a lower bound for $E_P(h)$ in terms of the solutions of a finite number of linear optimisation problems, one for each sector,

$$E_P^{\inf}(h) \geqslant 2\sum_\sigma A^\sigma \left(\max_{|\xi^{a\sigma} - \xi^{b\sigma}| \leqslant |\mathbf{v}^a - \mathbf{v}^b|} \sum_a \xi^{a\sigma} w^{a\sigma} \right). \tag{2.15}$$

A simpler characterisation is provided by the dual formulation,

$$E_P^{\inf}(h) \geqslant 2\sum_\sigma A^\sigma \left(\min_{\Omega^{ab,\sigma}} \sum_{a,b} \big|\mathbf{v}^a - \mathbf{v}^b\big| \Omega^{ab,\sigma} \right), \tag{2.16}$$

where the $\Omega^{ab,\sigma}$'s are constrained by

$$\sum_a \Omega^{ab,\sigma} = -w^{b\sigma}, \qquad \sum_b \Omega^{ab,\sigma} = w^{a\sigma}. \tag{2.17}$$

Let us fix σ. Without loss of generality, we can restrict $\Omega^{ab,\sigma}$ to be nonnegative and equal to zero unless $w^{a\sigma} > 0$ and $w^{b\sigma} < 0$. Suppose first that the nonzero wrapping numbers are either $+1$ or -1; by (1.11) there are an equal number, m say, of each. Therefore, the nonvanishing elements of $\Omega^{ab,\sigma}$ may be identified with an $m \times m$ matrix, which we denote by M. (2.17) implies that M is doubly stochastic. By a theorem of Birkhoff [2], M can be expressed as a convex linear combination of permutation matrices. Then the minimum in (2.16) is necessarily achieved at an extremal point, i.e. for M a permutation matrix corresponding to a minimal connection. In this case,

$$\min_{\Omega^{ab,\sigma}} \sum_{a,b} \big|\mathbf{v}^a - \mathbf{v}^b\big| \Omega^{ab,\sigma} = L\big(\mathcal{P}^\sigma(h), \mathcal{N}^\sigma(h)\big), \tag{2.18}$$

where $\mathcal{P}^\sigma(h)$ (resp. $N^\sigma(h)$) contains vertices $\mathbf{v}^a$ for which $w^{a\sigma}$ equals $+1$ (resp. -1). The case of general nonzero wrapping numbers values is treated by including $\mathbf{v}^a$ with multiplicity $|w^{a\sigma}|$ in either $\mathcal{P}^\sigma(h)$ (for $w^{a\sigma} > 0$) or $N^\sigma(h)$ (for $w^{a\sigma} < 0$). The same argument applies in every sector (there is a separate minimal connection for each σ), and (1.12) follows. □

3. Upper bound for rectangular prisms

Let P denote a rectangular prism centred at the origin of three-dimensional Euclidean space. We take the edges of P to be parallel to the coordinate axes and of lengths L_x, L_y, L_z, oriented so that $L_x \geqslant L_y \geqslant L_z$. It will be convenient to introduce the half-lengths

$$l_j = \frac{L_j}{2} \tag{3.1}$$

(here and in what follows, the index j takes values x, y or z). Then the vertices of P are of the form

$$\mathbf{v}^a = (\pm l_x, \pm l_y, \pm l_z), \tag{3.2}$$

where the vertex label a designates the signs in (3.2).

Let $O^a \subset S^2$ denote the spherical octant of directions about $\mathbf{v}^a$ which are contained in P. E.g., for $\mathbf{v}^a = (-l_x, -l_y, -l_z)$, O^a is the positive octant $\{\mathbf{s} \in S^2 \mid s_j \geqslant 0\}$. The boundary of O^a, ∂O^a, contains the directions which lie in the faces at $\mathbf{v}^a$, and is composed of quarter-segments of the great circles about $\hat{\mathbf{x}}$, $\hat{\mathbf{y}}$ and $\hat{\mathbf{z}}$. Let ∂O^a_j denote the segment about $\hat{\mathbf{j}}$.

Choose l so that $0 < l \leqslant l_z$. Then $\mathbf{v}^a + lO^a$ is contained in P, so that $\mathbf{v}^a + lO^a$ is a cleaved surface. Given $\mathbf{n} \in \mathcal{C}_P(h)$, we can define a unit-vector field $\boldsymbol{\nu}^a$ on O^a by

$$\boldsymbol{\nu}^a(\mathbf{s}) = \mathbf{n}\big(\mathbf{v}^a + l\mathbf{s}\big). \tag{3.3}$$

Tangent boundary conditions imply that, for $\mathbf{s} \in \partial O^a_j$, $\boldsymbol{\nu}^a(\mathbf{s})$ is orthogonal to $\hat{\mathbf{j}}$. Denote the set of $\boldsymbol{\nu}^a$'s collectively by $\boldsymbol{\nu}$. The wrapping numbers of $\mathbf{n}$, and hence its homotopy type, are determined by $\boldsymbol{\nu}$. $\boldsymbol{\nu}$ is an example of an *octant configuration*, which we define generally as follows:

Definition 3.1. An octant configuration $\boldsymbol{\nu}$ with admissible topology $h = \{w^{a\sigma}\}$ is a set of continuous piecewise-smooth maps $\boldsymbol{\nu}^a : O^a \to S^2$ satisfying tangent boundary conditions,

$$\mathbf{s} \in \partial O^a_j \Longrightarrow \boldsymbol{\nu}(\mathbf{s}) \cdot \hat{\mathbf{j}} = 0, \tag{3.4}$$

such that

$$\int_{O^a} \boldsymbol{\nu}^*\big(\chi^\sigma \omega\big) = w^{a\sigma} A^\sigma. \tag{3.5}$$

The Dirichlet energy of an octant configuration $\boldsymbol{\nu}$ on the octant O^a is defined by

$$E^a_{(2)}(\boldsymbol{\nu}) = \int_{O^a} \big(\nabla \boldsymbol{\nu}^a\big)^2(\mathbf{s})\, \mathrm{d}\Omega^a. \tag{3.6}$$

Here and in what follows, it will be convenient to regard $\nabla \nu^a_j(\mathbf{s})$ (the gradient of the jth component of $\boldsymbol{\nu}^a$) as a vector in $\mathbb{R}^3$ which is tangent to O^a at $\mathbf{s}$. $\mathrm{d}\Omega^a$ in (3.6) denotes the area element on O^a (normalised so that O^a has area $\pi/2$). The Dirichlet energy on the octant edge ∂O^a_j is given by

$$E^a_{(1)j}(\boldsymbol{\nu}) = \int_0^{\pi/2} \left(\frac{\mathrm{d}}{\mathrm{d}\alpha} \boldsymbol{\nu}^a\big(\mathbf{s}^a_j(\alpha)\big)\right)^2 \mathrm{d}\alpha. \tag{3.7}$$

Here, $\mathbf{s}^a_j(\alpha)$ denotes the parameterisation of ∂O^a_j by arclength (i.e., angle) α. For example, if $\mathbf{v}^a = (-l_x, -l_y, -l_z)$,

$$\mathbf{s}^a_j(\alpha) = \cos\alpha \hat{\mathbf{k}} + \sin\alpha \hat{\mathbf{l}}, \quad 0 \leqslant \alpha \leqslant \frac{\pi}{2}, \tag{3.8}$$

where (j, k, l) denote a triple of distinct indices.

By an *extension* of an octant configuration $\boldsymbol{\nu}$, we mean a continuous, piecewise-smooth unit-vector field $\mathbf{n}$ on P such that $\mathbf{n}(\mathbf{v}^a + l\mathbf{s}) = \boldsymbol{\nu}^a(\mathbf{s})$ for all $\mathbf{s} \in O^a$. Obviously, if $\boldsymbol{\nu}$ has topology h, so has its extension $\mathbf{n}$. We introduce the following notation: Given functions f and g on a domain W, we write $f \lesssim g$ to mean there exists a constant C such that $|f| \leqslant C|g|$ on W. In this case, we say that f is dominated by g.

Lemma 3.1. *Let $\boldsymbol{\nu}$ be an octant configuration with admissible topology h. Then $\boldsymbol{\nu}$ can be extended to a continuous piecewise-differentiable configuration $\mathbf{n} \in \mathcal{H}C_P(h)$ such that*

$$E(\mathbf{n}) \lesssim \kappa^3 L_z \biggl(\sum_a E^a_{(2)}(\boldsymbol{\nu}) + \sum_{aj} \bigl(E^a_{(1)j}(\boldsymbol{\nu})\bigr)^{1/2} \biggr). \tag{3.9}$$

Theorem 1.3 is proved by constructing octant configurations whose Dirichlet energies on the octants and their edges scale appropriately with the wrapping numbers. These configurations are provided by the following:

Lemma 3.2. *Given an admissible topology $h = \{w^{a\sigma}\}$, there exists an octant configuration $\boldsymbol{\nu}$ with topology h such that*

$$\sum_a E^a_{(2)}(\boldsymbol{\nu}) \lesssim \sum_{a\sigma} |w^{a\sigma}|, \tag{3.10}$$

$$\sum_{aj} E^a_{(1)j}(\boldsymbol{\nu}) \lesssim \sum_{a\sigma} |w^{a\sigma}|^2. \tag{3.11}$$

The proofs of Lemmas 3.1 and 3.2, which involve explicit constructions and estimates, are given in Sections 4 and 5 respectively.

Proof of Theorem 1.3. Given an admissible topology $h = \{w^{a\sigma}\}$, we choose an octant configuration $\boldsymbol{\nu}$ with topology h as in Lemma 3.2, and extend it to a unit-vector field $\mathbf{n}$ on P as in Lemma 3.1. From the Cauchy–Schwartz inequality, (3.11) implies that

$$\sum_{aj} \bigl(E^a_{(1)j}(\boldsymbol{\nu})\bigr)^{1/2} \lesssim \sum_{a\sigma} |w^{a\sigma}|. \tag{3.12}$$

Together, (3.9), (3.10) and (3.12) provide an estimate for $E(\mathbf{n})$, and therefore an upper bound for $E_P^{\inf}(h)$,

$$E_P^{\inf}(h) \leqslant E(\mathbf{n}) \lesssim \kappa^3 L_z \sum_{a\sigma} |w^{a\sigma}|. \tag{3.13}$$

From Theorem 1.2, a lower bound for $E_P^{\inf}(h)$ is given by

$$E_P^-(h) = \sum_\sigma 2\frac{\pi}{2} L\bigl(P^\sigma(h), N^\sigma(h)\bigr) \tag{3.14}$$

($A^\sigma = \pi/2$ for a rectangular prism). The minimum distance between vertices of P is L_z. As the number of elements of $P^\sigma(h)$ (and of $N^\sigma(h)$) is $\frac{1}{2}\sum_a |w^{a\sigma}|$, it follows that

$$L\bigl(P^\sigma(h), N^\sigma(h)\bigr) \geqslant \frac{1}{2} L_z \sum_a |w^{a\sigma}|. \tag{3.15}$$

From (3.13) and (3.15), we conclude that

$$E_P^{\inf}(h) \lesssim \kappa^3 E_P^-(h). \qquad \square \tag{3.16}$$

We remark that the octant configurations of Lemma 3.2 must be chosen with some care, as the following example illustrates (details may be found in [17]). For simplicity, take P to be the unit cube. In the (positive) octant about $\mathbf{v}^a = (-\frac{1}{2}, -\frac{1}{2}, -\frac{1}{2})$, let

$$\boldsymbol{\nu}^a(\theta, \phi) = (\sin\alpha \cos\beta, \sin\alpha \sin\beta, \cos\alpha), \tag{3.17}$$

where $0 \leqslant \theta, \phi \leqslant \pi/2$ and $\alpha = (4M+1)\theta$, $\beta = (4N+1)\phi$ for integers M and N. Given $(x, y, z) \in P$ with $x, y, z \leqslant 0$, let (θ, ϕ) denote the polar angles of (x, y, z) with respect to $\mathbf{v}^a$, and let $\mathbf{n}(x, y, z) = \boldsymbol{\nu}^a(\theta, \phi)$. We define $\mathbf{n}$ elsewhere via $\mathbf{n}(\pm x, y, z) = \mathbf{n}(x, \pm y, z) = \mathbf{n}(x, y, \pm z) = \mathbf{n}(x, y, z)$ (so that $\mathbf{n}$ is a reflection-symmetric configuration [18,20]).

Then $\mathbf{n}$ is continuous and satisfies tangent boundary conditions. Denote its homotopy class by h_{MN}. It is straightforward to compute the wrapping numbers (it turns out that they scale linearly with M and N), and, from Theorem 1.2, to obtain the following lower bound:

$$E_P^-(h_{MN}) = \big(2\max(M+2N, 2M+N)+1\big)\frac{\pi}{4}. \tag{3.18}$$

It turns out that $E(\mathbf{n})$ can be evaluated exactly as a finite sum of Appell hypergeometric functions. For large M and N, the energy is given asymptotically by

$$E(\mathbf{n}) \sim 4\sqrt{3}\left((4M+1)^2 + \frac{1}{2}\ln M(4N+1)^2\right)\frac{\pi}{2}. \tag{3.19}$$

Clearly $E(\mathbf{n})$ does not scale linearly with M and N, so is not dominated by the lower bound $E_P^-(h_{MN})$.

4. Extending octant configurations

Let us specify the geometry of the prism P in greater detail. Let

$$\mathbf{m}^a_{(j)} = \mathbf{v}^a - v^a_j\hat{\mathbf{j}} \tag{4.1}$$

denote the midpoint of the edge through $\mathbf{v}^a$ along $\hat{\mathbf{j}}$ (here, v^a_j is the jth component of $\mathbf{v}^a$). Let C^a denote the triangle whose vertices are the midpoints of the edges coincident at $\mathbf{v}^a$,

$$C^a = \left\{\mathbf{r} = \tau_x\mathbf{m}^a_{(x)} + \tau_y\mathbf{m}^a_{(y)} + \tau_z\mathbf{m}^a_{(z)} \;\middle|\; \tau_j \geqslant 0, \sum_j \tau_j = 1\right\}. \tag{4.2}$$

We call C^a a *cleaved face* (see Fig. 1). $\mathbf{c} \in C^a$ satisfies

$$\mathbf{C}^a \cdot \mathbf{c} = 2, \tag{4.3}$$

where

$$\mathbf{C}^a = \big((v^a_x)^{-1}, (v^a_y)^{-1}, (v^a_z)^{-1}\big) \tag{4.4}$$

is an (unnormalised) outward normal on C^a. Let h denote the distance from C^a to the origin. Then

$$\frac{2}{3}l_z \leqslant h = \frac{2}{|\mathbf{C}^a|} < 2l_z. \tag{4.5}$$

Let $F^{j\tau}$, where $\tau = \pm 1$, denote face of the prism which lies in the plane $\{r_j = \tau l_j\}$. Let $\widehat{F}^{j\tau} \subset F^{j\tau}$ denote the rhombus whose vertices lie at the midpoints of the edges of $F^{j\tau}$. We call $\widehat{F}^{j\tau}$ a *truncated face* (see Fig. 1).

We partition P into three sets of pyramids, denoted X^a, Y^a and $Z^{j\tau}$. X^a and Y^a have the cleaved face C^a as their (shared) base. X^a has its apex at $\mathbf{v}^a$, while Y^a has its apex at the origin. $Z^{j\tau}$ has the truncated face $\widehat{F}^{j\tau}$ as its base and its apex at the origin. Every point of P belongs either to the interior of just one of these pyramids or else to the boundary between two or more of them (see Fig. 1).

In the proof of Lemma 3.1, we define $\mathbf{n}$, the extension of the octant configuration $\boldsymbol{\nu}$, to be constant along rays from C^a to the origin (apart from a small neighbourhood thereof) and along rays to $\mathbf{v}^a$. We then show that the energy of $\mathbf{n}$ in X^a and Y^a is proportional to $E^a_{(2)}(\boldsymbol{\nu})$. The construction of $\mathbf{n}$ in $Z^{j\tau}$ is more complicated. On $\partial\widehat{F}^{j\tau}$ (the boundary of the base), $\mathbf{n}$ is determined by $\boldsymbol{\nu}$, and in the interior of $\widehat{F}^{j\tau}$, we define $\mathbf{n}$ by a simple interpolation which respects tangent boundary conditions. In the interior of $Z^{j\tau}$, we do *not* take $\mathbf{n}$ to be constant along rays from the apex to the base, as this would give rise to an energy proportional to $\sum_{\mathbf{v}^a\in F^{j\tau}} E^a_{(1)j}(\boldsymbol{\nu})$, which, for the octant configurations of Lemma 3.2, would scale as the square of the wrapping numbers. Instead, along such rays, and over a distance

$$\sigma = \left(\pi \sum_{\mathbf{v}^a\in F^{j\tau}} \big(E^a_{(1)j}(\boldsymbol{\nu})\big)\right)^{-1/2}, \tag{4.6}$$

$\mathbf{n}$ is rotated toward the normal $\hat{\mathbf{j}}$. This leads to an energy in $Z^{j\tau}$ proportional to $1/\sigma$.

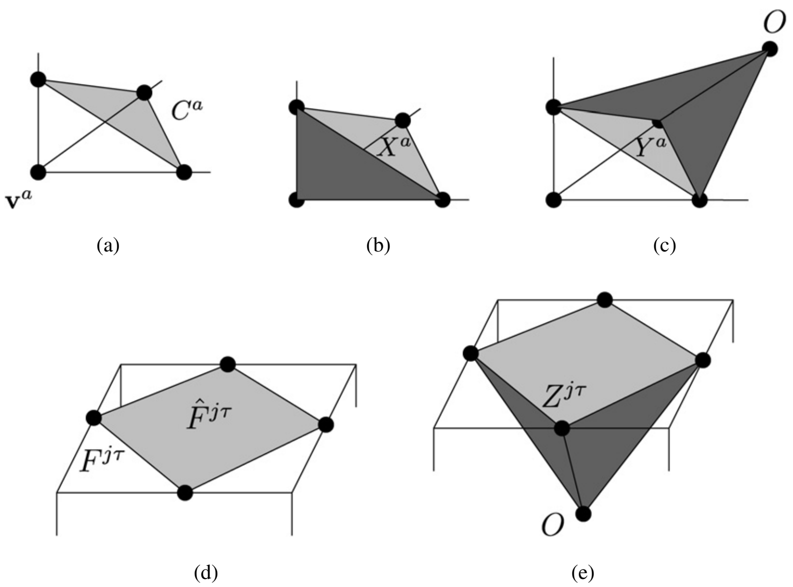

Fig. 1. (a) The cleaved plane C^a, (b) the pyramid X^a, (c) the pyramid Y^a, (d) the truncated face $F^{j\tau}$, (e) the pyramid $Z^{j\tau}$.

Proof of Lemma 3.1. Given an octant configuration $\boldsymbol{\nu}$, we define an extension $\mathbf{n}$ on the pyramids X^a, Y^a and $Z^{j\tau}$ (Steps 1–3) with Dirichlet energies $E_{X^a}(\mathbf{n})$, $E_{Y^a}(\mathbf{n})$ and $E_{Z^{j\tau}}(\mathbf{n})$ bounded as follows:

$$E_{X^a}(\mathbf{n}) \leqslant \frac{1}{2}\kappa L_z E^a_{(2)}(\boldsymbol{\nu}), \tag{4.7a}$$

$$E_{Y^a}(\mathbf{n}) \lesssim \kappa^3 L_z E^a_{(2)}(\boldsymbol{\nu}), \tag{4.7b}$$

$$E_{Z^{j\tau}}(\mathbf{n}) \lesssim \kappa^2 L_z \sum_{\mathbf{v}^a \in F^{j\tau}} \big(E^a_{(1)j}(\boldsymbol{\nu})\big)^{1/2}. \tag{4.7c}$$

Then

$$E(\mathbf{n}) = \sum_a \big(E_{X^a}(\mathbf{n}) + E_{Y^a}(\mathbf{n})\big) + \sum_{j\tau} E_{Z^{j\tau}}(\mathbf{n})$$
$$\lesssim \kappa^3 L_z \bigg(\sum_a E^a_{(2)}(\boldsymbol{\nu}) + \sum_{aj} \big(E^a_{(1)j}(\boldsymbol{\nu})\big)^{1/2}\bigg). \tag{4.8}$$

To ensure continuity (Step 4) we modify the construction of $\mathbf{n}$ near the origin while preserving the bounds (4.7).

Step 1. Construction in X^a. From (4.2) and (4.3), points in X^a are of the form $\mathbf{v}^a + r\mathbf{s}$, where $\mathbf{s} \in O^a$ and $0 < r \leqslant r^a(\mathbf{s})$ with

$$r^a(\mathbf{s}) = \frac{1}{|\mathbf{C}^a \cdot \mathbf{s}|}; \tag{4.9}$$

$r^a(\mathbf{s})$ is the distance from $\mathbf{v}^a$ to C^a along $\mathbf{s}$. The maximal distance is half the length of the longest edge, so that

$$r^a(\mathbf{s}) \leqslant r^a(\hat{\mathbf{x}}) = l_x. \tag{4.10}$$

We define $\mathbf{n}$ in X^a by

$$\mathbf{n}\big(\mathbf{v}^a + r\mathbf{s}\big) = \boldsymbol{\nu}^a(\mathbf{s}), \quad \mathbf{s} \in O^a,\ 0 < r \leqslant r^a(\mathbf{s}). \tag{4.11}$$

Then, from (3.6) and (4.10),

$$E_{X^a}(\mathbf{n}) := \int_{X^a} (\nabla \mathbf{n})^2 \,\mathrm{d}V = \int_{O^a} r^a(\mathbf{s})\big(\nabla \boldsymbol{\nu}^a(\mathbf{s})\big)^2 \,\mathrm{d}\Omega^a \leqslant l_x E^a_{(2)}(\boldsymbol{\nu}) \leqslant \frac{1}{2}\kappa L_z E^a_{(2)}(\boldsymbol{\nu}), \tag{4.12}$$

as in (4.7a).

Step 2. Construction in Y^a. Points in Y^a (excluding the origin) are of the form $\lambda\mathbf{c}$, where $\mathbf{c} \in C^a$ and $0 < \lambda \leqslant 1$. We define $\mathbf{n}$ in Y^a by

$$\mathbf{n}(\lambda\mathbf{c}) = \mathbf{n}(\mathbf{c}). \tag{4.13}$$

Note that $\mathbf{n}(\mathbf{c})$ is fixed in Step 1, since C^a belongs to X^a as well as Y^a.

To estimate $E_{Y^a}(\mathbf{n})$, we resolve $\nabla\mathbf{n}$ into components tangent and normal to the cleaved face C^a,

$$\nabla\mathbf{n} = \nabla_t\mathbf{n} + \nabla_n\mathbf{n}, \tag{4.14}$$

so that $(\mathbf{C}^a \cdot \nabla_t)\mathbf{n} = 0$ and $(\mathbf{t} \cdot \nabla_n)\mathbf{n} = 0$ for $\mathbf{t}$ tangent to C^a. From (4.13), $\nabla_t\mathbf{n}(\lambda\mathbf{c}) = \lambda^{-1}\nabla_t\mathbf{n}(\mathbf{c})$. Therefore,

$$\big(\nabla_t\mathbf{n}(\lambda\mathbf{c})\big)^2 = \frac{1}{\lambda^2}\big(\nabla_t\mathbf{n}(\mathbf{c})\big)^2. \tag{4.15}$$

To estimate $(\nabla_n\mathbf{n})^2$, we note that $(\mathbf{c} \cdot \nabla)\mathbf{n}(\lambda\mathbf{c}) = 0$ ($\mathbf{n}$ is constant along rays in Y^a through the origin) and resolve $\mathbf{c}$ into components $\mathbf{c}_t$ and $\mathbf{c}_n$ tangent and normal to C^a to obtain

$$\big(\nabla_n\mathbf{n}(\lambda\mathbf{c})\big)^2 \leqslant \frac{|\mathbf{c}_t|^2}{|\mathbf{c}_n|^2}\big(\nabla_t\mathbf{n}(\lambda\mathbf{c})\big)^2 \leqslant \frac{|\mathbf{c}_t|^2}{|\mathbf{c}_n|^2}\frac{1}{\lambda^2}\big(\nabla_t\mathbf{n}(\mathbf{c})\big)^2. \tag{4.16}$$

Since $(\nabla_t\mathbf{n}(\mathbf{c}))^2 \leqslant (\nabla\mathbf{n}(\mathbf{c}))^2$, (4.15) and (4.16) together give

$$\big(\nabla\mathbf{n}(\lambda\mathbf{c})\big)^2 = \frac{|\mathbf{c}|^2}{|\mathbf{c}_n|^2}\frac{1}{\lambda^2}\big(\nabla\mathbf{n}(\mathbf{c})\big)^2. \tag{4.17}$$

Clearly $|\mathbf{c}| \leqslant l_x$ while $|\mathbf{c}_n|$ is just h, the distance from C^a to the origin, and $h > 2l_z/3$ (cf. (4.5)), so that

$$\big(\nabla\mathbf{n}(\lambda\mathbf{c})\big)^2 \leqslant \frac{9}{4}\kappa^2\frac{1}{\lambda^2}\big(\nabla\mathbf{n}(\mathbf{c})\big)^2. \tag{4.18}$$

The volume element on Y^a is given by

$$\mathrm{d}V = h\lambda^2\,\mathrm{d}^2c\,\mathrm{d}\lambda, \tag{4.19}$$

where d^2c is the Euclidean area element on C^a. Since $h < 2l_z$,

$$E_{Y^a}(\mathbf{n}) = \int_{Y^a}(\nabla\mathbf{n})^2\,\mathrm{d}V < \frac{9}{2}\kappa^2 l_z\int_{C^a}(\nabla\mathbf{n})^2(\mathbf{c})\,\mathrm{d}^2c. \tag{4.20}$$

Letting $\mathbf{s} = (\mathbf{c} - \mathbf{v})/|\mathbf{c} - \mathbf{v}|$, we can write the preceding as an integral over O^a. We have that

$$\mathrm{d}^2c = \frac{|\mathbf{c}|^2}{|\mathbf{s}\cdot\mathbf{C}^a|/|\mathbf{C}^a|}\,\mathrm{d}\Omega^a, \qquad \big(\nabla\mathbf{n}(\mathbf{c})\big)^2 = \frac{1}{|\mathbf{c}|^2}\big(\nabla\boldsymbol{\nu}^a(\mathbf{s})\big)^2, \tag{4.21}$$

and

$$\frac{|\mathbf{C}^a|}{|\mathbf{s}\cdot\mathbf{C}^a|} < \frac{3/l_z}{1/l_x} = 3\kappa, \tag{4.22}$$

so that (4.20) becomes

$$E_{Y^a}(\mathbf{n}) \leqslant \frac{27}{2}\kappa^3 l_z\int_{O^a}\big(\nabla\boldsymbol{\nu}^a(\mathbf{s})\big)^2\,\mathrm{d}\Omega^a \lesssim \kappa^3 L_z E_2^a(\boldsymbol{\nu}), \tag{4.23}$$

as in (4.7b).

Step 3. Construction in $Z^{j\tau}$. To simplify the discussion and the notation, let us fix our attention on the top face of the prism, with $j = z$ and $\tau = 1$, and henceforth drop the designation $j\tau$, writing Z for $Z^{j\tau}$, $\widehat{F}$ for $\widehat{F}^{j\tau}$, etc, in what follows (the other faces are handled similarly). $\partial\widehat{F}$ may be parameterised as $\mathbf{R}(\phi) = (R(\phi)\cos\phi, R(\phi)\sin\phi, l_z)$, where

$$R(\phi) = \frac{l_x l_y}{l_y|\cos\phi| + l_x|\sin\phi|} \tag{4.24}$$

and ϕ is the polar angle about the z-axis. On $\partial\widehat{F}$ (which is also contained in the cleaved faces), $\mathbf{n}$ is defined in Step 1. It follows that $\mathbf{n}$ is continuous on $\partial\widehat{F}$ (including the midpoints of the edges of F, which belong to two cleaved faces, as $\boldsymbol{\nu}$ has an admissible topology) and satisfies tangent boundary conditions there. Tangent boundary conditions imply that

$$\mathbf{n}\big(\mathbf{R}(\phi)\big) = \epsilon\cos\big(\Theta(\phi)\big)\hat{\mathbf{y}} + \sin\big(\Theta(\phi)\big)\hat{\mathbf{x}}, \tag{4.25}$$

where $\Theta(\phi)$ may be taken to be continuous and piecewise smooth, with $\Theta(2\pi) - \Theta(0)$ equal to a multiple of 2π. Since $\boldsymbol{\nu}$ has an admissible topology, we must have $\Theta(2\pi) = \Theta(0)$. $\epsilon = \pm 1$ can be chosen so that

$$\Theta(0) = \Theta(2\pi) = 0. \tag{4.26}$$

We introduce polygonal cylindrical coordinates (h, ξ, ϕ) on Z, defined by

$$x = h\xi R(\phi)\cos\phi, \quad y = h\xi R(\phi)\sin\phi, \quad z = l_z h, \quad 0 < h \leqslant 1,\ 0 \leqslant \xi \leqslant 1,\ 0 \leqslant \phi < 2\pi. \tag{4.27}$$

ξ, the radial coordinate, is scaled to equal 1 on the sides of Z and 0 along the z-axis. Then let

$$\mathbf{N}_{(2)}(\xi, \phi) = \epsilon\cos(\xi\Theta)\hat{\mathbf{y}} + \sin(\xi\Theta)\hat{\mathbf{x}}. \tag{4.28}$$

$\mathbf{N}_{(2)}$ gives a continuous extension of $\mathbf{n}$ to the interior of $\widehat{F}$ which satisfies tangent boundary conditions. A continuous extension to the interior of Z is given by

$$\mathbf{N}(h, \xi, \phi) = \cos\gamma\,\mathbf{N}_{(2)} + \sin\gamma\,\hat{\mathbf{z}}, \tag{4.29}$$

where $\gamma = \gamma(h, \xi)$ is given by

$$\gamma(h, \xi) = \Phi\left(\frac{1-h}{\sigma}\right)\Phi\left(\frac{1-\xi}{\sigma}\right)\frac{\pi}{2}, \quad \Phi(s) = \begin{cases} s, & s < 1, \\ 1, & s \geqslant 1, \end{cases} \tag{4.30}$$

and $0 < \sigma < 1$. Thus, γ vanishes on the boundary of Z and has a constant value, $\pi/2$, at interior points sufficiently far from the boundary. σ, which determines how far, will be specified below. We define $\mathbf{n}$ on Z as

$$\mathbf{n}\big(x(h, \xi, \phi), y(h, \xi, \phi), z(h, \xi, \phi)\big) = \mathbf{N}(h, \xi, \phi). \tag{4.31}$$

It is readily checked that (4.31) agrees with (4.13) at points on the boundary of Z except at the origin.

The energy of $\mathbf{n}$ in Z is given by $E_Z(\mathbf{n})$ as follows. In terms of the coordinates (h, ξ, ϕ), we have that

$$\begin{aligned} E_Z(\mathbf{n}) &= \int_Z (\nabla\mathbf{n})^2\,\mathrm{d}V \\ &= \int_0^1 \mathrm{d}h \int_0^1 \mathrm{d}\xi \int_0^{2\pi} \mathrm{d}\phi \big|(\nabla\xi \times \nabla\phi)\cdot\nabla h\big|^{-1}(\mathbf{N}_h\nabla h + \mathbf{N}_\xi\nabla\xi + \mathbf{N}_\phi\nabla\phi)^2, \end{aligned} \tag{4.32}$$

where $\mathbf{N}_h = \partial\mathbf{N}/\partial h$, $\mathbf{N}_\xi = \partial\mathbf{N}/\partial\xi$, etc. From (4.28) and (4.29), we get that

$$\begin{aligned} \mathbf{N}_h &= \gamma_h(\cos\gamma\,\hat{\mathbf{z}} - \sin\gamma\,\mathbf{N}_{(2)}), \\ \mathbf{N}_\xi &= \gamma_\xi(\cos\gamma\,\hat{\mathbf{z}} - \sin\gamma\,\mathbf{N}_{(2)}) + \epsilon\Theta\cos\gamma\,\mathbf{N}_{(2)} \times \hat{\mathbf{z}}, \\ \mathbf{N}_\phi &= \epsilon\xi\Theta'\cos\gamma\,\mathbf{N}_{(2)} \times \hat{\mathbf{z}}. \end{aligned} \tag{4.33}$$

From (4.27), we get that

$$\begin{aligned} \nabla h &= (0, 0, 1/l_z), \\ \nabla\xi &= \xi\big((R\cos\phi + R'\sin\phi)/(\rho R), (R\sin\phi - R'\cos\phi)/(\rho R), -1/(l_z h)\big), \\ \nabla\phi &= (-\sin\phi, \cos\phi, 0)/\rho, \end{aligned} \tag{4.34}$$

where $\rho = (x^2 + y^2)^{1/2} = h\xi R$. Straightforward calculation then gives an expression for $E_Z(\mathbf{n})$ of the form

$$E_Z(\mathbf{n}) = \sum_{i=1}^5 \mathcal{E}_i = \sum_{i=1}^5 \int_0^1 \mathrm{d}h \int_0^1 \mathrm{d}\xi \int_0^{2\pi} \mathrm{d}\phi\, I_i, \tag{4.35}$$

where the integrands for the separate contributions $\mathcal{E}_i$ are given by

$$I_1 = l_z \cos^2\gamma \xi \Theta'^2, \qquad I_2 = \frac{h^2}{l_z}\gamma_h^2 \xi R^2, \qquad I_3 = -2\frac{h}{l_z}\gamma_h\gamma_\xi \xi^2 R^2,$$
$$I_4 = -2\epsilon l_z \cos^2\gamma \xi \frac{R'}{R}\Theta\Theta', \qquad I_5 = \left(l_z\xi\left(1+\frac{R'^2}{R^2}\right)+\frac{\xi^3}{l_z}R^2\right)\left(\cos^2\gamma\Theta^2+\gamma_\xi^2\right). \tag{4.36}$$

We consider these contributions in turn.

Concerning $\mathcal{E}_1$, since $\cos^2\gamma$ vanishes for $0<\xi, h<1-\sigma$ (cf. (4.30)), it follows that

$$\mathcal{E}_1 \leqslant 2l_z\sigma \int_0^{2\pi} \Theta'^2(\phi)\,\mathrm{d}\phi. \tag{4.37}$$

The integral of $\Theta'^2(\phi)$ can be related to the Dirichlet edge energies $E^a_{(1)z}(\boldsymbol{\nu})$ for the vertices $\mathbf{v}^a$ which lie on F. For convenience, label these anticlockwise by $a = 0, 1, 2, 3$ so that

$$\mathbf{n}\big(\mathbf{R}(\phi)\big) = \boldsymbol{\nu}^a\big(\mathbf{s}^a_z\big(\alpha(\phi)\big)\big), \quad (a-1)\pi/2 < \phi < a\pi/2, \tag{4.38}$$

where $\mathbf{s}^a_z(\alpha)$ parameterises the octant edge ∂O^a_z as in (3.8), and $\alpha(\phi)$ is given by

$$\tan\alpha = \begin{cases} (l_x/l_y)^2\tan\phi, & 0\leqslant\phi<\pi/2 \text{ or } \pi\leqslant\phi<3\pi/2,\\ (l_y/l_x)^2\tan\phi, & \pi/2\leqslant\phi<\pi \text{ or } 3\pi/2\leqslant\phi<2\pi. \end{cases} \tag{4.39}$$

(ϕ is the angle with respect to the centre of F and α, with $0<\alpha<\pi/2$, the angle with respect consecutive vertices. (4.39) gives the elementary relation between them. See also Fig. 2.) Recalling (4.25), we get that

$$\Theta'^2(\phi) = \left(\frac{\mathrm{d}}{\mathrm{d}\phi}\mathbf{n}\big(\mathbf{R}(\phi)\big)\right)^2 = \left(\frac{\mathrm{d}}{\mathrm{d}\alpha}\boldsymbol{\nu}^a\big(\mathbf{s}^a_z(\alpha)\big)\right)^2\bigg|_{\alpha=\alpha(\phi)}\left(\frac{\mathrm{d}\alpha}{\mathrm{d}\phi}\right)^2. \tag{4.40}$$

It follows that

$$\int_0^{2\pi}\Theta'^2(\phi)\,\mathrm{d}\phi = \sum_{\mathbf{v}^a\in F}\int_0^{\pi/2}\left(\frac{\mathrm{d}}{\mathrm{d}\alpha}\boldsymbol{\nu}^a\big(\mathbf{s}^a_z(\alpha)\big)\right)^2\left(\frac{\mathrm{d}\phi}{\mathrm{d}\alpha}\right)^{-1}\mathrm{d}\alpha. \tag{4.41}$$

From (4.39) one has that

$$\left|\left(\frac{\mathrm{d}\phi}{\mathrm{d}\alpha}\right)^{-1}\right| \leqslant \frac{l_x^2}{l_y^2} \leqslant \kappa^2. \tag{4.42}$$

Therefore,

$$\int_0^{2\pi}\Theta'^2(\phi)\,\mathrm{d}\phi \leqslant \kappa^2\sum_{\mathbf{v}^a\in F}E^a_{(1)z}(\boldsymbol{\nu}). \tag{4.43}$$

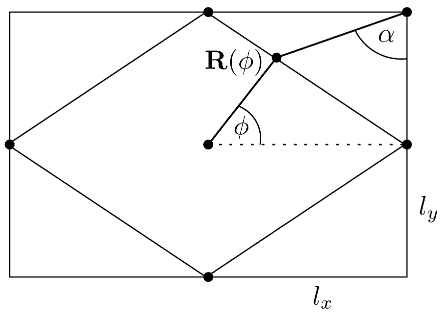

Fig. 2. The angles α and ϕ.

Substituting into (4.37), we get

$$\mathcal{E}_1 \lesssim \kappa^2 l_z \sigma \sum_{\mathbf{v}^a \in F} E^a_{(1)z}(\boldsymbol{v}). \tag{4.44}$$

Next we consider

$$\mathcal{E}_2 = \int_0^1 \mathrm{d}h \frac{h^2}{l_z} \int_0^1 \mathrm{d}\xi\, \xi \gamma_h^2 \int_0^{2\pi} \mathrm{d}\phi\, R^2. \tag{4.45}$$

From (4.24), $R(\phi) \leqslant l_x$, and from (4.30), $|\gamma_h|$ vanishes for $h < 1 - \sigma$ and is bounded by $\pi/(2\sigma)$ for $h > 1 - \sigma$. Therefore,

$$\mathcal{E}_2 < \frac{\pi^3}{4} \frac{l_x^2}{l_z} \frac{1}{\sigma} \lesssim \kappa^2 l_z \frac{1}{\sigma}. \tag{4.46}$$

We estimate $\mathcal{E}_3$ similarly; noting that $|\gamma_\xi|$ vanishes for $\xi < 1 - \sigma$ and is bounded by $\pi/(2\sigma)$ for $\xi > 1 - \sigma$, we obtain

$$|\mathcal{E}_3| \lesssim \kappa^2 l_z \frac{1}{\sigma}. \tag{4.47}$$

$\mathcal{E}_4$ is given by

$$\mathcal{E}_4 = -2\epsilon l_z \int_0^1 \mathrm{d}h \int_0^1 \mathrm{d}\xi\, \xi \cos^2\gamma \int_0^{2\pi} \mathrm{d}\phi\, \Theta\Theta' \frac{R'}{R}. \tag{4.48}$$

We consider the ϕ-integral first. From the Cauchy–Schwartz inequality,

$$\left| \int_0^{2\pi} \Theta\Theta' \frac{R'}{R} \mathrm{d}\phi \right| \leqslant \left(\int_0^{2\pi} \Theta^2 \mathrm{d}\phi \right)^{1/2} \left(\int_0^{2\pi} \Theta'^2 \left(\frac{R'}{R}\right)^2 \mathrm{d}\phi \right)^{1/2}. \tag{4.49}$$

In the first factor on the right-hand side, note that, from (4.25) and (4.38),

$$\left|\Theta(\phi)\right| \leqslant \sum_{\mathbf{v}^a \in F} \int_0^{\pi/2} \left| \left(\frac{\mathrm{d}}{\mathrm{d}\alpha} \boldsymbol{v}^a\big(\mathbf{s}^a_z(\alpha)\big) \right) \right| \mathrm{d}\alpha, \quad \text{for } 0 \leqslant \phi \leqslant 2\pi. \tag{4.50}$$

The Cauchy–Schwartz inequality then implies that

$$\Theta^2(\phi) \leqslant 2\pi \sum_{\mathbf{v}^a \in F} E^a_{(1)z}(\boldsymbol{v}), \quad \text{for } 0 \leqslant \phi \leqslant 2\pi. \tag{4.51}$$

In the second factor on the right-hand side of (4.49), we have that $|R'/R| \leqslant \kappa$ (cf. (4.24)), so it follows from (4.43) that

$$\int_0^{2\pi} \Theta'^2 \left(\frac{R'}{R}\right)^2 \mathrm{d}\phi \leqslant \kappa^4 \sum_{\mathbf{v}^a \in F} E^a_{(1)z}(\boldsymbol{v}). \tag{4.52}$$

Substituting (4.51) and (4.52) into (4.49), we get that

$$\left| \int_0^{2\pi} \Theta\Theta' \frac{R'}{R} \mathrm{d}\phi \right| \lesssim \kappa^2 \sum_{\mathbf{v}^a \in F} E^a_{(1)z}(\boldsymbol{v}). \tag{4.53}$$

We substitute (4.53) into (4.48) and recall that $\cos^2\gamma$ vanishes for $0 < \xi, h < 1 - \sigma$ to get that

$$|\mathcal{E}_4| \lesssim \kappa^2 l_z \sigma \sum_{\mathbf{v}^a \in F} E^a_{(1)z}(\boldsymbol{v}). \tag{4.54}$$

Finally, we consider

$$\mathcal{E}_5 = \int_0^1 \mathrm{d}h \int_0^1 \mathrm{d}\xi \int_0^{2\pi} \mathrm{d}\phi \left(\cos^2\gamma\,\Theta^2 + \gamma_\xi^2\right)\left(l_z\xi\left(1 + \frac{R'^2}{R^2}\right) + \frac{\xi^3}{l_z}R^2\right). \tag{4.55}$$

Let us first estimate the ϕ-dependent terms. From (4.24), we have that $R \leqslant \kappa l_z$ and $|R'/R| \leqslant \kappa$, while (4.51) provides a bound for $\Theta^2(\phi)$. Substituting into (4.55), we get that

$$\mathcal{E}_5 \leqslant 2\pi l_z \int_0^1 \mathrm{d}h \int_0^1 \mathrm{d}\xi \left(2\pi\cos^2\gamma \sum_{\mathbf{v}^a\in F} E^a_{(1)z}(\boldsymbol{\nu}) + \gamma_\xi^2\right)\left(\xi\left(1+\kappa^2\right) + \xi^3\kappa^2\right). \tag{4.56}$$

Recalling that $\cos^2\gamma$ and γ_ξ^2 vanish for $0 < \xi, h < 1-\sigma$ while γ_ξ^2 is bounded by $\pi/(2\sigma)$, we obtain the bound

$$\begin{aligned}\mathcal{E}_5 &\leqslant 4\pi l_z\sigma\left(2\pi\sum_{\mathbf{v}^a\in F} E^a_{(1)z}(\boldsymbol{\nu}) + \frac{\pi^2}{4\sigma^2}\right)\left(1+2\kappa^2\right)\\ &\lesssim \kappa^2 l_z\sigma\left(\sum_{\mathbf{v}^a\in F} E^a_{(1)z}(\boldsymbol{\nu})\right) + \kappa^2 l_z\frac{1}{\sigma}.\end{aligned} \tag{4.57}$$

We substitute the estimates (4.37), (4.46), (4.47), (4.54) and (4.56) for $\mathcal{E}_i$ into (4.35), and take

$$\sigma = \left(\pi\sum_{\mathbf{v}^a\in F} E^a_{(1)z}(\boldsymbol{\nu})\right)^{-1/2}. \tag{4.58}$$

We can verify that $\sigma < 1$ as follows: Tangent boundary conditions imply that, for ϕ a multiple of $\pi/2$ (i.e., for $\mathbf{R}(\phi)$ belonging to an edge of F), $\Theta(\phi) = \pi/2 \bmod 2\pi$. Then (4.51) implies that

$$\sum_{\mathbf{v}^a\in F} E^a_{(1)z} \geqslant \frac{\pi}{8},$$

so that $\sigma < \sqrt{8}/\pi < 1$. Then (4.57) and (4.58) give

$$E_Z \lesssim \kappa^2 l_z\left(\sum_{\mathbf{v}^a\in F} E^a_{(1z)}\right)^{1/2} \lesssim \kappa^2 l_z \sum_{\mathbf{v}^a\in F}\left(E^a_{(1z)}\right)^{1/2}, \tag{4.59}$$

as in (4.7c). The same estimate may be carried out for the other pyramids $Z^{j\tau}$. Different lengths l_j appear as appropriate, but since ratios of lengths are bounded by κ, (4.59) holds generally.

Step 4. Continuity. As defined, $\mathbf{n}$ is continuous everywhere except at the origin. Here we modify $\mathbf{n}$ in a small neighbourhood of the origin to remove the discontinuity while preserving the estimate (4.7).

From the definitions (4.13) and (4.31) of $\mathbf{n}$ in Y^a and $Z^{j\tau}$, $\mathbf{n}(\mathbf{r})$ is radially constant in the ball B_δ about the origin of radius $\delta = (1-\sigma)l_z$. Let $\boldsymbol{\gamma}: S^2 \to S^2$ denote the restriction of $\mathbf{n}$ to ∂B_δ, given by

$$\boldsymbol{\gamma}(\mathbf{s}) = \mathbf{n}(\delta\mathbf{s}), \quad \mathbf{s}\in S^2. \tag{4.60}$$

Let

$$E_{(2)}(\boldsymbol{\gamma}) = \int_{S^2} (\nabla\boldsymbol{\gamma})^2\,\mathrm{d}\Omega \tag{4.61}$$

denote the Dirichlet energy of $\boldsymbol{\gamma}$. Then, for $0 < \epsilon < 1$, the energy of $\mathbf{n}$ in the $\epsilon\delta$-ball about the origin is given by

$$E_{B_{\epsilon\delta}}(\mathbf{n}) = \epsilon\delta E_{(2)}(\boldsymbol{\gamma}). \tag{4.62}$$

$\boldsymbol{\gamma}$ is piecewise smooth, and, since $\boldsymbol{\nu}$ has an admissible topology, of degree zero. It follows that $\boldsymbol{\gamma}$ is smoothly homotopic to a constant map. Let $\boldsymbol{\Gamma}_s$ denote a homotopy, so that $\boldsymbol{\Gamma}_1(\mathbf{s}) = \boldsymbol{\gamma}(\mathbf{s})$ and $\boldsymbol{\Gamma}_0(\mathbf{s}) = \mathbf{s}_0$. Let $\mathbf{g}$ be the unit-vector field on B_δ given by

$$\mathbf{g}(r\mathbf{s}) = \boldsymbol{\Gamma}_{r/\delta}(\mathbf{s}), \tag{4.63}$$

and let $E_{B_\delta}(\mathbf{g})$ denote its Dirichlet energy. For $0<\epsilon<1$, we define $\mathbf{g}_\epsilon$ to be the unit-vector field on $B_{\epsilon\delta}$ given by

$$\mathbf{g}_\epsilon(\mathbf{r}) = \mathbf{g}(\mathbf{r}/\epsilon). \tag{4.64}$$

Then the energy of $\mathbf{g}_\epsilon$ in the $\epsilon\delta$-ball about the origin is given by

$$E_{B_{\epsilon\delta}}(\mathbf{g}_\epsilon) = \epsilon E_{B_\delta}(\mathbf{g}). \tag{4.65}$$

For any $0<\epsilon<1$ we can redefine $\mathbf{n}$ on $B_{\epsilon\delta}$, taking it to be $\mathbf{g}_\epsilon$ there, and leaving $\mathbf{n}$ unchanged elsewhere. It is clear that $\mathbf{n}$ as redefined is continuous and piecewise smooth. From (4.62) and (4.65), the redefinition changes its energy by $\epsilon(E_{B_\delta}(\mathbf{g}) - \delta E_{(2)}(\boldsymbol{\gamma}))$. As ϵ can be made arbitrarily small, the estimates (4.7) remain valid. □

5. Constructing octant configurations

For definiteness, we consider the configuration on a particular octant, namely the positive octant about the vertex $(-l_x, -l_y, -l_y)$; the treatment for the other octants is analogous. To simplify the notation, we will drop the vertex label a. Hence, throughout this section, we write $O = \{\mathbf{s} \in S^2 \mid s_j \geqslant 0\}$ for the positive octant (instead of O^a), $\boldsymbol{\nu}: O \to S^2$ for the configuration on O (instead of $\boldsymbol{\nu}^a$), w^σ instead of $w^{a\sigma}$, etc. With reference to (3.6) and (3.7), we let

$$E_{(2)}(\boldsymbol{\nu}) = \int_O (\nabla \boldsymbol{\nu})^2(\mathbf{s})\,\mathrm{d}\Omega, \tag{5.1}$$

$$E_{(1)j}(\boldsymbol{\nu}) = \int_0^{\pi/2} \left(\frac{\mathrm{d}\boldsymbol{\nu}}{\mathrm{d}\alpha}\right)^2 \big(\mathbf{s}_j(\alpha)\big)\,\mathrm{d}\alpha, \tag{5.2}$$

where $\mathrm{d}\Omega$ denotes the area element on O and

$$\mathbf{s}_j(\alpha) = \cos\alpha\,\hat{\mathbf{k}} + \sin\alpha\,\hat{\mathbf{l}} \tag{5.3}$$

denotes the parameterisation of ∂O_j. Lemma 3.2 follows from showing that

$$E_{(2)}(\boldsymbol{\nu}) \lesssim \sum_\sigma |w^\sigma|, \tag{5.4}$$

$$\sum_j E_{(1)j}(\boldsymbol{\nu}) \lesssim \sum_\sigma |w^\sigma|^2, \tag{5.5}$$

as analogous relations hold for the other octants. Before establishing (5.4) and (5.5) in Section 5.3, we first review the topological characterisation of octant configurations (Section 5.1) and their representation by complex functions, particularly conformal representatives (Section 5.2).

5.1. Topological characterisation

As discussed in [24] (in the context of general convex polyhedra) and in [18,20] (for a rectangular prism), the homotopy class of $\boldsymbol{\nu}: O \to S^2$ may be characterised by certain invariants, namely the *edge signs*, denoted $e = (e_x, e_y, e_z)$, *kink numbers*, denoted $k = (k_x, k_y, k_z)$ and *trapped area*, denoted Ω. Here we recall the definitions of these invariants and some relevant results for prisms; details may be found in the references.

Tangent boundary conditions imply that $\boldsymbol{\nu}(\hat{\mathbf{j}})$ is parallel to $\hat{\mathbf{j}}$; the edge sign e_j determines their relative sign, i.e.

$$\boldsymbol{\nu}(\hat{\mathbf{j}}) = e_j \hat{\mathbf{j}}. \tag{5.6}$$

Tangent boundary conditions also imply that along $\mathbf{s}_j(\alpha)$, $\boldsymbol{\nu}$ takes values in the (kl)-plane. The integer-valued kink number k_j counts the number of windings of $\boldsymbol{\nu}$ in this plane relative to the minimum possible winding (a net rotation of $\pm\pi/2$), for which $k_j = 0$. The trapped area Ω is the oriented area of the image of $\boldsymbol{\nu}$, given by

$$\Omega = \int_O \boldsymbol{\nu}^*\omega. \tag{5.7}$$

For a rectangular prism, the sectors are octants of S^2 labelled by a triple of signs $\sigma = (\sigma_x, \sigma_y, \sigma_z)$, with $S^\sigma = \{\mathbf{s} \in S^2 \mid \operatorname{sgn}(\mathbf{s}\cdot\hat{\mathbf{j}}) = \sigma_j\}$. The wrapping numbers w^σ may be expressed in terms of (e, k, Ω), as follows [24,20]:

$$w^\sigma = \frac{1}{4\pi}\Omega + \frac{1}{2}\sum_j \sigma_j k_j + \frac{1}{8}e_*(1 - 8\delta_{\sigma e}), \tag{5.8}$$

where $\delta_{\sigma e}$ equals one if $\sigma = e$ and is zero otherwise. Note that (5.8) implies that

$$\Omega = -2\pi \sum_j \sigma_j k_j - e_*\pi/2 \mod 4\pi, \tag{5.9}$$

where

$$e_* = e_x e_y e_z. \tag{5.10}$$

(5.8) may be inverted to obtain (e, k, Ω) in terms of the wrapping numbers,

$$e_t = -\sum_\sigma \sigma_r \sigma_s w^\sigma, \quad \text{for } r, s, t \text{ distinct}, \tag{5.11}$$

$$k_r = \frac{1}{4}\sum_\sigma \sigma_r w^\sigma + \frac{1}{4}e_r e_*, \tag{5.12}$$

$$\Omega = \sum_\sigma \frac{\pi}{2} w^\sigma. \tag{5.13}$$

(Similar relations are described for a general polyhedron in Appendix A.)

A topology for a prism configuration $\mathbf{n}$ may be specified as a set of edge signs, kink numbers and trapped areas for each vertex. The conditions for the topology to be admissible (i.e., realisable by a configuration continuous away from the vertices) are readily expressed in terms of (e, k, Ω); pairs of edge signs associated with a single edge must be compatible, the absence of surface singularities implies sum rules for the kink numbers on each face of the prism, and the absence of interior singularities implies a sum rule for the trapped areas.

We say that an octant topology (e, k, Ω) is *conformal* (resp. *anticonformal*) if every nonzero wrapping number is negative (resp. positive). From (5.8), one can show that (e, k, Ω) is conformal (resp. anticonformal) if and only if $\Omega \leqslant -\Omega_-(e, k)$ (resp. $\Omega \geqslant \Omega_+(e, k)$), where

$$\begin{aligned}
\Omega_{e_*}(e, k) &= 2\pi \sum_j |k_j| + 2\pi \begin{cases} +\frac{7}{4}, & \text{if } e_* e_j k_j \leqslant 0 \text{ for all } j, \\ -\frac{1}{4}, & \text{otherwise.} \end{cases} \\
\Omega_{-e_*}(e, k) &= 2\pi \sum_j |k_j| - 2\pi \begin{cases} +\frac{7}{4}, & \text{if } e_* e_j k_j > 0 \text{ for all } j, \\ -\frac{1}{4}, & \text{otherwise.} \end{cases}
\end{aligned} \tag{5.14}$$

If (Ω, e, k) is an octant topology, then Ω differs from $\Omega_+(e, k)$ or $\Omega_-(e, k)$ by some multiple of 4π (i.e., some number of whole coverings of the sphere). If $\Omega = \Omega_\pm(e, k)$, then (e, k, Ω) has at least one wrapping number equal to zero.

5.2. Conformal configurations

$\boldsymbol{\nu} : O \to S^2$ can be represented by a complex function $F(w, \overline{w})$ in the standard way via the stereographic projection $S^2 \to \mathbb{C}^*$ ($\mathbb{C}^*$ is the extended complex plane),

$$F\left(\frac{s_x + \mathrm{i}s_y}{1 + s_z}, \frac{s_x - \mathrm{i}s_y}{1 + s_z}\right) = \left(\frac{\nu_x + \mathrm{i}\nu_y}{1 + \nu_z}\right)(\mathbf{s}). \tag{5.15}$$

The domain of F is the positive quarter-unit disk (the image of O under the projection),

$$Q = \{w \in \mathbb{C} \mid 0 \leqslant \operatorname{Re} w \leqslant 1,\ 0 \leqslant \operatorname{Im} w \leqslant 1,\ |w| \leqslant 1\}. \tag{5.16}$$

Letting $w_j(\alpha)$ denote the projections of the parameterised boundaries $\mathbf{s}_j(\alpha)$ of ∂O_j, we have that

$$w_x(\alpha) = \tan(\alpha/2), \quad w_y(\alpha) = \mathrm{i}\bigl(1 - \tan(\alpha/2)\bigr), \quad w_z = \mathrm{e}^{\mathrm{i}\alpha}. \tag{5.17}$$

A standard calculation gives

$$(\nabla \boldsymbol{\nu})^2 = 4\frac{|F_{\overline{w}}|^2 + |F_w|^2}{(1+|F|^2)^2}, \tag{5.18}$$

so that (cf. (5.1) and (5.2))

$$E_{(2)}(\boldsymbol{\nu}) = \int_Q 4\frac{|\partial_{\overline{w}} F|^2 + |\partial_w F|^2}{(1+|F|^2)^2}\,\mathrm{d}^2 w, \tag{5.19}$$

$$E_{(1)j}(\boldsymbol{\nu}) = \int_0^{\pi/2} 4\left(\frac{|\partial_{\overline{w}} F|^2 + |\partial_w F|^2}{(1+|F|^2)^2}\right)\bigl(w_j(\alpha)\bigr)\left|\frac{\mathrm{d}w_j}{\mathrm{d}\alpha}(\alpha)\right|^2 \mathrm{d}\alpha. \tag{5.20}$$

Of particular interest are configurations for which F is conformal (a function of w only) or anticonformal. For definiteness we will consider the conformal case, and write $F(w,\overline{w}) = f(w)$. If f has a meromorphic extension to the extended complex plane, then tangent boundary conditions imply that f is real when w is real, f is imaginary when w is imaginary, and $|f| = 1$ when $|w| = 1$. It follows that if w_* is a zero of f, then so are $-w_*$ and $\pm\overline{w}_*$, while $\pm 1/w_*$ and $\pm 1/\overline{w}_*$ are poles. Therefore, f is in fact a rational function of the form

$$f = \lambda w^n ABC. \tag{5.21}$$

Here, A contains the real zeros and poles of f, B the imaginary zeros and poles, and C the strictly complex zeros and poles. n is an odd integer giving the order of the zero or pole at the origin, and $\lambda = \pm 1$ is an overall sign. A, B and C may be written explicitly as

$$A(w) = \prod_{j=1}^{a}\left(\frac{w^2 - r_j^2}{r_j^2 w^2 - 1}\right)^{\rho_j}, \tag{5.22a}$$

$$B(w) = \prod_{k=1}^{b}\left(\frac{w^2 + s_k^2}{s_k^2 w^2 + 1}\right)^{\sigma_k}, \tag{5.22b}$$

$$C(w) = \prod_{l=1}^{c}\left(\frac{(w^2 - t_l^2)(w^2 - \bar{t}_l^2)}{(t_l^2 w^2 - 1)(\bar{t}_l^2 w^2 - 1)}\right)^{\tau_l}. \tag{5.22c}$$

Here, a is the number of real zeros and poles in Q (excluding the origin), b the number of imaginary zeros and poles in Q (excluding the origin), and c the number of strictly complex zeros and poles in Q. r_j, with $0 < r_j < 1$, denotes the real zeros ($\rho_j = 1$) and poles ($\rho_j = -1$); similarly, $\mathrm{i}s_k$, with $0 < s_k < 1$ and $\sigma_k = \pm 1$, denote the imaginary zeros and poles, and t_l, with $0 < |t_l| < 1$, $\mathrm{Re}\, t_l, \mathrm{Im}\, t_l > 0$ and $\tau_l = \pm 1$ denote the strictly complex zeros and poles.

In terms of these parameters, the edge signs, kink numbers and trapped area of conformal configurations are given by [18,20]

$$e_x = \lambda(-1)^a, \quad e_y = \lambda(-1)^b(-1)^{(n-1)/2}, \quad e_z = \operatorname{sgn} n, \tag{5.23}$$

$$\begin{aligned} k_x &= -\frac{1}{2}(-1)^b e_y\left(\sum_{k=1}^{b}(-1)^k\sigma_k + \frac{1}{2}\bigl(1-(-1)^b\bigr)e_z\right),\\ k_y &= -\frac{1}{2}(-1)^a e_x\left(\sum_{j=1}^{a}(-1)^j\rho_j + \frac{1}{2}\bigl(1-(-1)^a\bigr)e_z\right),\\ k_z &= \frac{1}{4}(e_x e_y - n) - \frac{1}{2}\sum_{j=1}^{a}\rho_j - \frac{1}{2}\sum_{k=1}^{b}\sigma_k - \sum_{l=1}^{c}\tau_l, \end{aligned} \tag{5.24}$$

$$\Omega = -\frac{1}{2}\big(|n| + 2(a+b) + 4c\big)\pi. \tag{5.25}$$

The expressions for the edge signs follow from evaluating f at 1, i and 0, while the formula for Ω follows from noting that 8Ω is just (-4π times) the degree of f, which for a meromorphic function is the number of its zeros counted with multiplicity. The formulas for the kink numbers require a bit more calculation; details are given in [20].

It is easily checked that a conformal configuration $f(w)$ has a conformal octant topology (f is orientation-preserving, which implies that the nonzero wrapping numbers are negative). Therefore, octant topologies which are neither conformal nor anticonformal, i.e. (e,k,Ω) for which $-\Omega_-(e,k) < \Omega < \Omega_+(e,k)$, cannot be realised by $F = f(w)$ or $F = f(\overline{w})$. In [20] we establish a converse result, namely that every conformal (resp. anticonformal) octant topology has a conformal (resp. anticonformal) representative.

5.3. Proof of Lemma 3.2

Proof. Given an admissible topology h for P, let (e,k,Ω) denote the associated octant topology on O with wrapping numbers w^σ. We construct $\boldsymbol{v}$, or rather its complex representative $F(w,\overline{w})$, with topology (e,k,Ω) in Step 1. We establish the estimate (5.4) for $E_{(2)}(\boldsymbol{v})$ in Step 2. We then show that

$$E_{(1)j}(\boldsymbol{v}) \lesssim 1 + k_j^2 \tag{5.26}$$

for $j = z$ (Step 3) and $j = x, y$ (Step 4). From (5.9), $\Omega \neq 0$. (5.13) then implies that the wrapping numbers cannot all vanish, so that, from (5.12),

$$\sum_j 1 + |k_j|^2 \lesssim \sum_\sigma \left|w^\sigma\right|^2. \tag{5.27}$$

The bound (5.5) for $\sum_j E_{(1)j}(\boldsymbol{v})$ then follows from (5.26) and (5.27).

Step 1. Definition of F. In general, the octant topology (e,k,Ω) is neither conformal nor anticonformal. We will take F to be conformal outside a small disk in Q with conformal topology (e,k,Ω_*). Inside the disk, F is made to cover the complex plane $(\Omega - \Omega_*)/(4\pi)$ times; this will ensure that F has the required topology.

Let

$$\Omega_* = -2\pi\left(\sum_j |k_j| + 1 - \frac{3}{4}e_*\right). \tag{5.28}$$

Using (5.14), one can check that Ω_* is equal to either $-\Omega_-(e,k)$ or $-(\Omega_-(e,k) - 4\pi$; in either case, (e,k,Ω_*) is a conformal octant topology. Denoting its wrapping numbers by w_*^σ, it follows that $w_*^\sigma \leqslant 0$ and, from (5.8) and (5.14), that at least one of its wrapping numbers either vanishes or is equal to -1;

$$\left|w_*^{\sigma_0}\right| \leqslant 1 \quad \text{for some } \sigma_0. \tag{5.29}$$

An explicit conformal representative $f(w)$ with octant topology (e,k,Ω_*) of the form (5.21) and (5.22) is obtained by taking

$$\begin{aligned}
&n = (2-e_*)e_z, \qquad \lambda = e_x,\\
&a = 2|k_y|, \quad \rho_j = -(-1)^j e_x \operatorname{sgn} k_y, \quad 1 \leqslant j \leqslant a,\\
&b = 2|k_x|, \quad \sigma_k = -(-1)^k e_y \operatorname{sgn} k_x, \quad 1 \leqslant k \leqslant b,\\
&c = |k_z| + \frac{1}{2}(1-e_*), \qquad \tau_l = \begin{cases} -\operatorname{sgn} k_z, & l \leqslant |k_z|,\\ -e_z, & l = |k_z|+1,\end{cases}
\end{aligned} \tag{5.30}$$

as can be verified from (5.23)–(5.25). (The reason for introducing Ω_* – we could use $-\Omega_-(e,k)$ instead – is that conformal representatives for $(e,k,-\Omega_-(e,k))$ entail several special cases.) Let

$$4\pi m = \Omega - \Omega_*(e,k). \tag{5.31}$$

Then, from (5.9), m is an integer, and from (5.8),

$$w^\sigma = w_*^\sigma + m. \tag{5.32}$$

If $m = 0$, we let

$$F(w, \overline{w}) = f(w). \tag{5.33}$$

Otherwise, let w_0 denote a regular point of f in the interior of Q, and let $D_\epsilon(w_0)$ denote the open ϵ-disk about w_0. Choose ϵ sufficiently small so that $D_{2\epsilon}(w_0)$ is contained in Q and contains no poles of f. Let

$$s(w, \overline{w}) = \frac{|w - w_0| - \epsilon}{\epsilon} \tag{5.34}$$

(so that s varies between 0 and 1 as $|w - w_0|$ varies between ϵ and 2ϵ). Then for $m > 0$ we define

$$F(w, \overline{w}) = \begin{cases} f(w), & |w - w_0| \geqslant 2\epsilon, \\ sf(w) + (1-s)(f(w_0) + (w - w_0)^m), & \epsilon < |w - w_0| < 2\epsilon, \\ f(w_0) + \epsilon^{2m}(\overline{w} - \overline{w}_0)^{-m}, & |w - w_0| \leqslant \epsilon, \end{cases} \tag{5.35a}$$

while for $m < 0$ we define

$$F(w, \overline{w}) = \begin{cases} f(w), & |w - w_0| \geqslant 2\epsilon, \\ sf(w) + (1-s)(f(w_0) + (\overline{w} - \overline{w}_0)^{-m}), & \epsilon < |w - w_0| < 2\epsilon, \\ f(w_0) + \epsilon^{-2m}(w - w_0)^{m}, & |w - w_0| \leqslant \epsilon. \end{cases} \tag{5.35b}$$

F coincides with f on ∂Q, so that F has the same edge signs and kink numbers as f, namely e and k. Let us verify that F has trapped area Ω. For $m = 0$ this is automatic. Otherwise, for definiteness, suppose that $m > 0$ (the case $m < 0$ is treated similarly). From (5.7) and (5.15) one can show that

$$\Omega(F) = \int_Q 4\frac{|\partial_{\overline{w}} F|^2 - |\partial_w F|^2}{(1 + |F|^2)^2}\, \mathrm{d}^2 w. \tag{5.36}$$

Divide the domain of integration as in (5.35). The contribution from $|w - w_0| > 2\epsilon$ is, to $\mathrm{O}(\epsilon^2)$, just the trapped area of f, namely $\Omega_*(e, k)$. Consider next the contribution from $D_\epsilon(w_0)$. From (5.35), $F(D_\epsilon(w_0))$ covers the extended complex plane m times with positive orientation, apart from an ϵ^m-disk about $f(w_0)$. It follows that its contribution to the integral in (5.36) is, to within $\mathrm{O}(\epsilon^{2m})$ corrections, $4\pi m$. The remaining contribution, from the annulus $D_{2\epsilon}(w_0) - D_\epsilon(w_0)$, is $\mathrm{O}(\epsilon^2)$. This is because the area of the annulus is $\mathrm{O}(\epsilon^2)$, while the integrand in (5.36) may be bounded independently of ϵ (since, by assumption, f has no poles in $D_{2\epsilon}(w_0)$). Since the trapped area is an odd multiple of $\pi/2$ (cf. (5.9)), it follows that, for small enough ϵ, F has trapped area $\Omega_*(e, k) + 4\pi m = \Omega$.

Clearly the topology of F does not depend on the positions of the zeros and poles of f. As will be evident in Step 2 below, neither does the octant energy $E_{(2)}(\boldsymbol{\nu})$, at least to leading order in ϵ. However, the edge energies, $E_{(1)j}(\boldsymbol{\nu})$, do depend on the positions of the zeros and poles. As will be evident in Steps 3 and 4, to obtain good control of the edge energies, the a real and b imaginary zeros and poles in Q should be kept away from the origin, the unit circle and each other, while the c strictly complex zeros and poles should be kept close to the unit circle and away from the real and imaginary axes and each other. Anticipating these requirements, in (5.22) we take

$$r_j = \frac{1}{4} + \frac{j}{2a}, \quad s_k = \frac{1}{4} + \frac{k}{2b}, \quad t_l = \left(1 - \frac{1}{c+1}\right)^{1/2} \mathrm{e}^{\mathrm{i}\alpha_l}, \quad \frac{\alpha_l}{\pi} = \frac{1}{8} + \frac{l}{4(c+1)}. \tag{5.37}$$

These imply the properties

$$\frac{1}{4} < r_j \leqslant \frac{3}{4}, \quad r_{j+1} - r_j = \frac{1}{2a}, \tag{5.38a}$$

$$\frac{1}{4} < s_k \leqslant \frac{3}{4}, \quad s_{k+1} - s_k = \frac{1}{2b}, \tag{5.38b}$$

$$\frac{\pi}{8} < \alpha_l \leqslant \frac{3\pi}{8}, \quad 1 - |t_l|^2 = \frac{1}{c+1} \tag{5.38c}$$

which will be useful in what follows. We note that, with r_j and ρ_j as given in (5.30) and (5.37), the real zeros and poles of f alternate along the interval $(0, 1]$; similarly, with s_k and σ_k as given in (5.30) and (5.37), the imaginary zeros and poles alternate along $(0, \mathrm{i}]$.

Step 2. Estimate of $E_{(2)}(\boldsymbol{\nu})$. The expression (5.19) for $E_{(2)}(\boldsymbol{\nu})$ differs from the expression (5.36) for Ω only in the relative sign of the w- and $\overline{w}$-derivative terms. Arguing as for (5.36), we see that, to order ϵ^2, the contributions to $E_{(2)}(\boldsymbol{\nu})$ from $Q - D_{2\epsilon}(w_0)$, $D_{2\epsilon}(w_0) - D_\epsilon(w_0)$, and $D_\epsilon(w_0)$ are, respectively, $|\Omega_*|$, 0 and $4\pi|m|$. Therefore,

$$E_{(2)}(\boldsymbol{\nu}) \lesssim |\Omega_*| + 4\pi|m| = \sum_\sigma \left|w_*^\sigma\right| \frac{\pi}{2} + 4\pi|m|, \tag{5.39}$$

where we have used (5.13) and the fact that $w_*^\sigma \leqslant 0$. From (5.32), $|w_*^\sigma| \leqslant |w^\sigma| + |m|$. Also, from (5.29) and (5.32), $|m| = |w^{\sigma_0} - w_*^{\sigma_0}| \leqslant |w^{\sigma_0}| + 1 \leqslant 2\sum_\sigma |w^\sigma|$. Substituting these results into (5.39), we get that

$$E_{(2)}(\boldsymbol{\nu}) \lesssim \sum_\sigma \left|w^\sigma\right|. \tag{5.40}$$

verifying (5.4).

Step 3. Estimate of $E_{(1)z}(\boldsymbol{\nu})$. On ∂O_z, $F = f$ and $|f| = 1$. Also, from (5.17), $|\mathrm{d}w_z/\mathrm{d}\alpha| = 1$. Therefore, from (5.20),

$$E_{(1)z}(\boldsymbol{\nu}) = \int_0^{\pi/2} \left|\frac{f'}{f}\right|^2 \left(\mathrm{e}^{\mathrm{i}\alpha}\right) \mathrm{d}\alpha. \tag{5.41}$$

Below we show that

$$\left|\frac{f'}{f}\right| \left(\mathrm{e}^{\mathrm{i}\alpha}\right) \lesssim 1 + |k_z|, \tag{5.42}$$

which then yields the required estimate (5.26) for $j = z$.

To verify (5.42), we note that, from (5.21),

$$\left|\frac{f'}{f}\right| = |n| + \left|\frac{A'}{A}\right| + \left|\frac{B'}{B}\right| + \left|\frac{C'}{C}\right|. \tag{5.43}$$

From the expression (5.22a) for A and the positions (5.38a) of its zeros and poles one calculates that

$$\frac{A'}{A}(w) = \pm\frac{w}{a} \sum_{J=1}^{a/2} \left(\frac{r_{2J-1} + r_{2J}}{(w^2 - r_{2J-1}^2)(w^2 - r_{2J}^2)} + \frac{r_{2J-1} + r_{2J}}{(r_{2J-1}^2 w^2 - 1)(r_{2J}^2 w^2 - 1)} \right). \tag{5.44}$$

From (5.38a), $|r_{2J} + r_{2J-1}| \leqslant 3/2$ while, for $w \in \partial O_z$, we have that $|w^2 - r_j^2|, |r_j^2 w^2 - 1| \geqslant 1/16$. Therefore,

$$\left|\frac{A'}{A}\right|(w) \lesssim \sum_{J=1}^{a/2} \frac{1}{a} \lesssim 1, \quad w \in \partial O_z. \tag{5.45}$$

A similar calculation (cf. (5.22b) and (5.38b)) shows that

$$\left|\frac{B'}{B}\right|(w) \lesssim 1, \quad w \in \partial O_z. \tag{5.46}$$

It remains to estimate C'/C. Without loss of generality, we may assume that $c > 0$ (otherwise, $C = 1$ and $C' = 0$). From (5.22c) and (5.38c),

$$\frac{C'}{C}\left(\mathrm{e}^{\mathrm{i}\alpha}\right) = 2\mathrm{e}^{-\mathrm{i}\alpha} \frac{1}{c+1} \sum_{l=1}^{c} \tau_l \left(\frac{(1 + |t_l|^2)}{|\mathrm{e}^{2\mathrm{i}\alpha} - t_l^2|^2} + \frac{(1 + |t_l|^2)}{|\mathrm{e}^{2\mathrm{i}\alpha} - \bar{t}_l^2|^2} \right). \tag{5.47}$$

Write the denominators (5.47) as

$$\begin{aligned} \left|\mathrm{e}^{2\mathrm{i}\alpha} - \bar{t}_l^2\right|^2 &= \left(1 - |t_l|^2\right)^2 + 4|t_l|^2 \sin^2(\alpha_l + \alpha), \\ \left|\mathrm{e}^{2\mathrm{i}\alpha} - t_l^2\right|^2 &= \left(1 - |t_l|^2\right)^2 + 4|t_l|^2 \sin^2(\alpha_l - \alpha). \end{aligned} \tag{5.48}$$

From (5.38c), one has that $1 - |t_l|^2 = 1/(c+1)$ while, for $0 \leqslant \alpha \leqslant \pi/2$, we have that $\pi/8 \leqslant \alpha + \alpha_l \leqslant 7\pi/8$ and $-\pi/2 < \alpha - \alpha_l < \pi/2$, so that

$$\left|e^{2i\alpha}-\bar{t}_l^2\right|^2 \geqslant \sin^2\left(\frac{\pi}{8}\right),$$
$$\left|e^{2i\alpha}-t_l^2\right|^2 \geqslant \frac{1}{(c+1)^2}+\frac{8}{\pi^2}(\alpha_l-\alpha)^2 \tag{5.49}$$

(we have used $(\pi/2)\sin|x| > |x|$ for $|x| \leqslant \pi/2$). Substituting (5.49) into (5.47) and using $\alpha_l = \pi/8 + l\pi/(4(c+1))$ (cf. (5.37)) and $1+|t_l|^2 < 2$ (cf. (5.38c)), we get that

$$\left|\frac{C'}{C}\left(e^{i\alpha}\right)\right| \leqslant \frac{2}{c+1}\sum_{l=1}^{c}\left(\frac{2(c+1)^2}{1+\frac{1}{2}(l-(c+1)(4\alpha/\pi-\frac{1}{2}))^2}+\frac{2}{\sin^2\pi/8}\right)$$
$$\lesssim (c+1)\sum_{l=0}^{c}\frac{1}{1+l^2}+1 \lesssim c+1. \tag{5.50}$$

We substitute (5.45), (5.46) and (5.50) into (5.43) to get that $|f'/f| \lesssim c+1+|n|$ on ∂O_z. Since c is equal to $|k_z|$ or $|k_z|+1$ and $|n| \leqslant 3$ (cf. (5.30)), the required estimate (5.42) follows.

Step 4. Estimate of $E_{(1)x}(\boldsymbol{v})$ and $E_{(1)y}(\boldsymbol{v})$. We establish (5.26) for $j=x$ and $j=y$. For definiteness, we consider $E_{(1)x}(\boldsymbol{v})$, and show that

$$E_{(1)x}(\boldsymbol{v}) \lesssim 1+|k_x|^2 \tag{5.51}$$

(the calculations for $E_{(1)y}(\boldsymbol{v})$ are essentially the same). On ∂O_x, $F=f$, f is real and, from (5.17), $dw_x/d\alpha = \frac{1}{2}\sec^2\alpha/2 \leqslant 1$ for $0 \leqslant \alpha \leqslant \pi/2$. It will be convenient to parameterise ∂O_x by $0 \leqslant w \leqslant 1$ rather than by α. (5.17) and (5.20) give that

$$E_{(1)x}(\boldsymbol{v}) = 4\int_0^1 \frac{f'^2}{(1+f^2)^2}\left|\frac{dw_x}{d\alpha}\right| dw \leqslant 4\int_0^1 \frac{f'^2}{(1+f^2)^2}\,dw. \tag{5.52}$$

The estimate (5.51) requires more calculation than the corresponding result for $j=z$. It turns out that a pointwise bound on the integrand in (5.52) is not sufficient, as $f'^2/(1+f^2)^2 \gtrsim |k_x|^3$ on ∂O_x. The domain on which $f'^2/(1+f^2)^2 \gtrsim |k_x|^3$ has measure of order $1/|k_x|$, in keeping with (5.51). But it will be necessary to estimate the integral in (5.52) itself. We note in passing that the complex representation (5.15) does not incorporate the cubic symmetries of the octant O in a simple way. Projecting along the axis $(1,1,1)/\sqrt{3}$ rather than $\hat{\mathbf{z}}$ would treat the boundaries symmetrically, and might lead to a simplification of the calculations below.

To proceed, we collect the zeros and poles of f along ∂O_x into a factor q (see (5.61) below for its explicit expression), writing

$$f = pq, \tag{5.53}$$

where

$$p = \tilde{A}BC = \lambda\prod_{j=1}^{a}\left(\frac{w+r_j}{r_j^2w^2-1}\right)^{\rho_j}BC \tag{5.54}$$

has no zeros or poles for $0 \leqslant w \leqslant 1$. We have that

$$\left|\frac{f'}{1+f^2}\right| = \left|\frac{p'}{p(pq+1/(pq))}+p\frac{q'}{1+p^2q^2}\right| \leqslant \frac{1}{2}\left|\frac{p'}{p}\right|+\max\left(|p|,\frac{1}{|p|}\right)\left|\frac{q'}{1+q^2}\right|, \tag{5.55}$$

since $|pq|+1/|pq| \geqslant 2$, and

$$1+p^2q^2 \geqslant \begin{cases} 1+q^2, & |p| \geqslant 1,\\ p^2(1+q^2), & |p| \leqslant 1. \end{cases} \tag{5.56}$$

With calculations similar to those in Step 3 (details are omitted), one shows that $|(\log p)'|$ is bounded on ∂O_x independently of k_j, i.e.

$$\left|\frac{p'}{p}\right| \lesssim 1, \quad 0 \leqslant w \leqslant 1. \tag{5.57}$$

From (5.22) and (5.54), if $a = 0$ then $p(0) = \pm 1$, i.e. $\log|p(0)| = 0$. If $a \neq 0$, using (5.37) we get that

$$\bigl|\bigl(\log\bigl|p(0)\bigr|\bigr)\bigr| = \sum_{J=1}^{a/2}\left|\log\frac{r_{2J-1}}{r_{2J}}\right| = \sum_{J=1}^{a/2}\bigl|\log\bigl(1-2/(a+4J)\bigr)\bigr| < \sum_{J=1}^{a/2} 4/(a+4J) < \int_0^{2a} \mathrm{d}x/(a+x) \leqslant \ln 3, \tag{5.58}$$

so that, in general, $|(\log|p(0)|)| \lesssim 1$. Then (5.57) and (5.58) imply that, for $0 \leqslant w \leqslant 1$,

$$\bigl|\bigl(\log\bigl|p(w)\bigr|\bigr)\bigr| \leqslant \bigl|\log\bigl(\bigl|p(0)\bigr|\bigr)\bigr| + \int_0^w |p'/p|\,\mathrm{d}w' \lesssim 1,$$

or

$$\max\bigl(|p|, 1/|p|\bigr) \lesssim 1, \quad 0 \leqslant w \leqslant 1. \tag{5.59}$$

Substituting (5.59) and (5.57) into (5.55), we get that

$$\left|\frac{f'}{1+f^2}\right| \lesssim 1 + \left|\frac{q'}{1+q^2}\right|. \tag{5.60}$$

The explicit form of q is obtained from (5.21), (5.22a) and (5.53),

$$q = w^n \prod_{j=1}^{a}(w-r_j)^{\rho_j}. \tag{5.61}$$

We partition ∂O_x into intervals whose endpoints are the zeros and poles of q and estimate $q'/(1+q^2)$ on each. We consider in detail the interval $I_J = (r_{2J-1}, r_{2J})$; the other intervals are treated similarly. Let $x = 2a(w - r_{2J-1})$, so that x varies between 0 and 1 on I_J. On I_J, we write

$$q\bigl(w(x)\bigr) = w^n(x)\bigl(g_J(x)h(x)\bigr)^{\rho_{2J-1}}, \tag{5.62}$$

where

$$h(x) = \frac{x}{x-1} \tag{5.63}$$

contains the zero and pole at the endpoints of I_J (an explicit expression for $g_J(x)$ is given in (5.70) below). It is straightforward to show (the calculation is similar to that in (5.55)) that

$$\left|\frac{q'}{1+q^2}\bigl(w(x)\bigr)\right| \leqslant \frac{1}{2}|n| + \left(\frac{\mathrm{d}w}{\mathrm{d}x}\right)^{-1}\left(\frac{1}{2}\left|\frac{\mathrm{d}g_J/\mathrm{d}x}{g_J}\right| + \left|\frac{g_J\,\mathrm{d}h/\mathrm{d}x}{1+g_J^2h^2}\right|\right). \tag{5.64}$$

Substituting (5.64) into (5.60) and noting that $|n| \leqslant 3$, $\mathrm{d}w/\mathrm{d}x = 1/(2a)$ and $\mathrm{d}h/\mathrm{d}x = -1/(1-x)^2$, we get that

$$\frac{f'^2}{(1+f^2)^2} \lesssim 1 + a^2\left|\frac{\mathrm{d}g_J/\mathrm{d}x}{g_J}\right|^2 + a^2\frac{1}{((1-x)^2/|g_J| + x^2|g_J|)^2}. \tag{5.65}$$

The integral of the last term in (5.65) may be estimated as follows:

$$\int_0^1 \bigl((1-x)^2/|g_J| + x^2|g_J|\bigr)^{-2}\,\mathrm{d}x \lesssim G_J + \mathcal{G}_J^{-1}, \tag{5.66}$$

where

$$\mathcal{G}_J = \min_{x\in[0,1]} |g_J|, \qquad G_J = \max_{x\in[0,1]} |g_J|. \tag{5.67}$$

To get (5.66), suppose first that $\mathcal{G}_J < 1 < G_J$. We divide [0, 1] into the three subintervals

$$K = \left[0, \frac{1}{2}G_J^{-1}\right], \quad L = \left[\frac{1}{2}G_J^{-1}, 1 - \frac{1}{2}\mathcal{G}_J\right], \quad M = \left[1 - \frac{1}{2}\mathcal{G}_J, 1\right]. \tag{5.68}$$

On K, the integrand in (5.66) is bounded by $G_J^2(1-x)^{-4}$, so that the contribution from K to the integral is dominated by G_J. On L, the integrand is bounded by $(2(1-x)x)^{-2}$ (since, in general, $|a/g| + |bg| \geqslant 2|ab|^{1/2}$), so the contribution from L is dominated by $G_J + \mathcal{G}_J^{-1}$. On M, the integrand is bounded by $g_J^{-2}x^{-4}$, so its contribution is dominated by $\mathcal{G}_J^{-1}$. In case $G_J < 1$, let $K = [0, \frac{1}{2}]$ and $L = [\frac{1}{2}, 1 - \mathcal{G}_J/2]$; in case $\mathcal{G}_J > 1$, let $L = [\frac{1}{2}G_J^{-1}, \frac{1}{2}]$ and $M = [\frac{1}{2}, 1]$.

From (5.65) and (5.66) it follows that

$$\int_{r_{2J-1}}^{r_{2J}} \frac{f'^2}{(1+f^2)^2}\,\mathrm{d}w \lesssim 1 + a \max_{0\leqslant x\leqslant 1}\left|\frac{\mathrm{d}g_J/\mathrm{d}x}{g_J}\right|^2 + a\big(G_J + \mathcal{G}_J^{-1}\big). \tag{5.69}$$

We need to estimate the terms involving g_J. From (5.61) and (5.62), g_J is given by

$$g_J(x) = P_{J-1}^{-1}(x)P_{a/2-J}(1-x), \tag{5.70}$$

where

$$P_N(x) = \prod_{K=1}^{N} \frac{x+2K-1}{x+2K} = \frac{\Gamma(N+\frac{1}{2}x+\frac{1}{2})}{\Gamma(N+\frac{1}{2}x+1)}\frac{\Gamma(\frac{1}{2}x+1)}{\Gamma(\frac{1}{2}x+\frac{1}{2})}. \tag{5.71}$$

Then leading-order asymptotics for $\Gamma(z)$, i.e. $\log\Gamma(z) \sim (z-\frac{1}{2})\log z - z$ and $(\log\Gamma)'(z) \sim \ln z$ (see, e.g., [1]), yields

$$P_N(x) \lesssim N^{-1/2} \quad \text{and} \quad \left|\frac{P_N'}{P_N}\right|(x) \lesssim 1 \quad \text{for } 0 \leqslant x \leqslant 1, \tag{5.72}$$

which in turn imply the estimates

$$\begin{aligned} &\left|\frac{\mathrm{d}g_J/\mathrm{d}x}{g_J}\right| \lesssim 1, \quad 0 \leqslant x \leqslant 1, \\ &G_J, \mathcal{G}_J^{-1} \lesssim \begin{cases} ((a/2+1-J)/J)^{1/2}, & 1 \leqslant J < a/4, \\ (J/(a/2+1-J))^{1/2}, & a/4 \leqslant J \leqslant a/2. \end{cases} \end{aligned} \tag{5.73}$$

Substituting (5.73) into (5.69), we get that

$$\int_{r_{2J-1}}^{r_{2J}} \frac{f'^2}{(1+f^2)^2}\,\mathrm{d}w \lesssim 1 + a + a\left(\frac{a/2+1-J}{J}\right)^{1/2} + a\left(\frac{J}{a/2+1-J}\right)^{1/2}. \tag{5.74}$$

Estimating the contribution from the interval $[r_{2J}, r_{2J+1}]$ to the integral (5.65) is carried out in much the same way. The differences are that (i) $h(x)$ is replaced by $1/h(x) = -h(1-x)$ (which may be accommodated by the substitution $x \to 1-x$) and (ii) $g_J(x)$ in (5.70) is replaced by

$$\frac{x+2J-1}{x+2J-a}P_{J-1}(x)P_{a/2-J-1}^{-1}(1-x). \tag{5.75}$$

But the expression in (5.75) and its logarithmic derivative satisfy the same bounds as do g_J and $\mathrm{d}g_J/\mathrm{d}x$ in (5.73). Thus, the integral of $f'^2/(1+f^2)^2$ over $[r_{2J}, r_{2J+1}]$ satisfies the same bound (5.74) as does the integral over $[r_{2J-1}, r_{2J}]$. We obtain a bound on the collective contribution from the intervals $[r_j, r_{j+1}]$ by summing over J in (5.74),

$$\int_{r_1}^{r_a} \frac{f'^2}{(1+f^2)^2}\,\mathrm{d}w \lesssim 1 + a^2 + a\sum_{J=1}^{a/2}\left(\frac{a/2+1-J}{J}\right)^{1/2} + a\sum_{J=1}^{a/2}\left(\frac{J}{a/2+1-J}\right)^{1/2}. \tag{5.76}$$

The first sum may be estimated as

$$\sum_{J=1}^{a/2}\left(\frac{a/2+1-J}{J}\right)^{1/2} \lesssim \int_0^{a/2}\left(\frac{a/2-y}{y}\right)^{1/2}\mathrm{d}y = \frac{a}{2}\int_0^1\left(\frac{1-s}{s}\right)^{1/2}\mathrm{d}s = \frac{\pi}{4}a, \tag{5.77}$$

and the second is similarly bounded. Thus

$$\int_{r_1}^{r_a} \frac{f'^2}{(1+f^2)^2}\,\mathrm{d}w \lesssim 1+a^2. \tag{5.78}$$

The contributions from the remaining intervals $[0, r_1]$ and $[r_a, 1]$ are treated similarly, and we get

$$\int_{0}^{r_1} \frac{f'^2}{(1+f^2)^2}\,\mathrm{d}w \lesssim 1+a^2, \tag{5.79}$$

$$\int_{r_a}^{1} \frac{f'^2}{(1+f^2)^2}\,\mathrm{d}w \lesssim 1+a^2. \tag{5.80}$$

We give an argument for (5.79) ((5.80) is treated similarly). For definiteness, let us assume that $\rho_1 = 1$ (the case $\rho_1 = -1$ is treated similarly). On $[0, r_1]$ we write $q = uv$, where $v = w^n(w - r_1)$ contains the zeros at the endpoints and

$$u = (w - r_a)^{-1} P^{-1}_{a/2-1}\left(1 - 2a\left(w - \frac{1}{4}\right)\right) \tag{5.81}$$

contains the remaining factors. Arguing as in (5.64) and (5.60) (but noting that u and v are functions of w, not a rescaled coordinate x), we get that

$$\frac{f'^2}{(1+f^2)^2} \lesssim 1 + \frac{u'^2}{u^2} + \frac{u^2 v'^2}{(1+u^2v^2)^2}. \tag{5.82}$$

Clearly $v'^2 \lesssim 1$, so that $u^2v'^2/(1+u^2v^2)^2 \lesssim u^2$. From (5.72) and (5.81), $|u'/u|^2 \lesssim a^2$ and $|u|^2 \lesssim a$. Therefore, $f'^2/(1+f^2)^2 \lesssim 1+a^2$, and (5.80) follows. The required bound on $E_{(1)x}(\boldsymbol{v})$, (5.51), follows from substituting the estimates (5.78)–(5.80) into the formula (5.52). □

Remark. To extend the upper bound of Theorem 3 to, say, a general convex polyhedron, one would like to have a generalisation of the octant configurations of Section 5.2. These would be conformal maps, perhaps with singularities, of a general convex geodesic polygon $\Sigma \subset S^2$ into S^2 such that each edge of Σ is mapped into the geodesic which contains it.

Acknowledgements

We thank CJ Newton and A Geisow for stimulating our interest in this area. AM was partially supported by an EPSRC/Hewlett-Packard Industrial CASE Studentship. AM and MZ were partially supported by EPSRC grant EP/C519620/1.

Appendix A. Wrapping numbers as complete invariants

In [24] we gave a homotopy classification of tangent unit-vector fields on a convex polyhedron P in terms of a set of invariants called edges signs, kink numbers and trapped areas. Here we show that these invariants can be determined from the wrapping numbers, so that the wrapping numbers $w^{a\sigma}$ constitute a complete set of invariants.

It suffices to consider the invariants associated with a single vertex. Let f be the number of faces of P. Let $\mathbf{v}$ denote a vertex of P, and let w^σ denote the wrapping numbers on a cleaved surface around $\mathbf{v}$ (we suppress the vertex label a), where σ is an f-tuple of signs. Suppose $\mathbf{v}$ has $b \geqslant 3$ coincident faces and therefore b coincident edges. Let E^r, $1 \leqslant r \leqslant b$, denote the edges coincident at $\mathbf{v}$, ordered consecutively clockwise with respect to a ray from $\mathbf{v}$ through the interior of P. By convention let $E^{b+1} = E^1$. Let $\mathbf{E}^r$ denote the unit vector along E^r directed away from $\mathbf{v}$. Let F^r denote the face with edges E^r and E^{r+1}. An (unnormalised) outward normal on F^r is given by

$$\mathbf{F}^r = \mathbf{E}^{r+1} \times \mathbf{E}^r. \tag{A.1}$$

Let us explain briefly how the edge signs, kink numbers and trapped areas are defined (see [24] for details). Fix a homotopy class $\mathcal{C}(h)$, and let $\mathbf{n} \in \mathcal{C}(h)$ denote a representative. The edge sign e^r is given by the orientation of $\mathbf{n}$ along the edge E^r relative to $\mathbf{E}^r$, so that $\mathbf{n}(\mathbf{r}) = e^r \mathbf{E}^r$ for $\mathbf{r} \in E^r$. The kink number k^r is an integer giving the winding number of $\mathbf{n}$ about $\mathbf{F}^r$ along a path on the face F^r starting on the edge E^{r+1} and ending on the edge E^r (tangent boundary conditions imply that $\mathbf{n}$ is orthogonal to $\mathbf{F}^r$ along such path). A minimal winding (e.g., $\mathbf{n}$ taking values along the shortest arc from $\mathbf{E}^{r+1}$ to $\mathbf{E}^r$ on S^2) has kink number equal to zero. Finally, the trapped area Ω is the area in S^2 of the image under $\mathbf{n}$ of a cleaved surface about $\mathbf{v}$ (the area is normalised so that S^2 has area 4π).

It is straightforward to derive the following expression for the wrapping numbers in terms of e^r, k^r and Ω [24]:

$$\Omega = 4\pi w^{\sigma(\mathbf{s})} + 2\pi \sum_{r=1}^{b} \operatorname{sgn}(\mathbf{F}^r \cdot \mathbf{s}) k^r + \sum_{r=2}^{b-1} \Big(A\big(e^1\mathbf{E}^1, e^r\mathbf{E}^r, e^{r+1}\mathbf{E}^{r+1}\big) - 4\pi \tau\big(\mathbf{s}; e^1\mathbf{E}^1, e^r\mathbf{E}^r, e^{r+1}\mathbf{E}^{r+1}\big)\Big). \tag{A.2}$$

Here, $\mathbf{s} \in S^2$ may be taken to be any unit vector which is transverse to every face of P (including faces which are not coincident at $\mathbf{v}$). $\sigma(\mathbf{s})$ gives the sector to which $\mathbf{s}$ belongs. For $\mathbf{a}, \mathbf{b}, \mathbf{c} \in S^2$, the quantities $A(\mathbf{a}, \mathbf{b}, \mathbf{c})$ and $\tau(\mathbf{s}; \mathbf{a}, \mathbf{b}, \mathbf{c})$ are defined as follows. Let $K \subset S^2$ denote the spherical triangle with vertices $\mathbf{a}$, $\mathbf{b}$, and $\mathbf{c}$ (K is well defined provided $\mathbf{a}$, $\mathbf{b}$ and $\mathbf{c}$ are not coplanar and no pair of them are antipodal). Then $A(\mathbf{a}, \mathbf{b}, \mathbf{c})$ is the oriented area of K with values between $-\pi$ and π (the sign is given by $\operatorname{sgn}(\mathbf{a} \cdot (\mathbf{b} \times \mathbf{c}))$). The quantity $\tau(\mathbf{s}; \mathbf{a}, \mathbf{b}, \mathbf{c})$ is given by

$$\tau(\mathbf{s}; \mathbf{a}, \mathbf{b}, \mathbf{c}) = \begin{cases} \operatorname{sgn}(\mathbf{a} \cdot (\mathbf{b} \times \mathbf{c})), & \mathbf{s} \in K, \\ 0, & \mathbf{s} \notin K. \end{cases} \tag{A.3}$$

That is, $\tau(\mathbf{s}; \mathbf{a}, \mathbf{b}, \mathbf{c})$ is equal to zero unless $\mathbf{s}$ belongs to K, in which case it is equal to ± 1 according to whether K has positive or negative area. Note that $\tau(\mathbf{s}; \mathbf{a}, \mathbf{b}, \mathbf{c})$ is well defined if $\mathbf{s}$ is transverse to the planes spanned by $\mathbf{a}, \mathbf{b}, \mathbf{c}$ taken pairwise.

Our task here is to show that, given the wrapping numbers w^σ for topology h, we can determine the edge signs, kink numbers and trapped areas. We begin by determining the edge signs, specifically e^r and e^{r+1}. Without loss of generality, we can assume that $r \neq 1$ and $r \neq b$ (note that (A.2) remains valid if the edge indices are cyclically permuted; there is nothing special about the edge E^1).

Let $S \subset S^2$ denote the great circle containing $\mathbf{E}^r$ and $\mathbf{E}^{r+1}$. The four points $\pm\mathbf{E}^r$, $\pm\mathbf{E}^{r+1}$ partition S into four disjoint open arcs. Denote these by S_m, $m = 1, 2, 3, 4$ (the ordering is not important). Let S_{m_*} denote the arc whose endpoints are $e^r\mathbf{E}^r$ and $e^{r+1}\mathbf{E}^{r+1}$. We determine m_*, and hence e^r and e^{r+1}, by means of the following calculation. For each m, choose some $\mathbf{s}_m \in S_m$, and let

$$\mathbf{s}_m^\pm = \mathbf{s}_m \pm \epsilon \mathbf{F}^r \tag{A.4}$$

(recall that $\mathbf{F}^r$ is normal to S) with $\epsilon > 0$ small enough so that $\mathbf{s}_m^\pm$ is transverse to every face of P and so that

$$\operatorname{sgn}\big(\mathbf{F}^s \cdot \mathbf{s}_m^+\big) = \operatorname{sgn}\big(\mathbf{F}^s \cdot \mathbf{s}_m^-\big), \quad s \neq r. \tag{A.5}$$

We subtract the two equations obtained by letting $\mathbf{s} = \mathbf{s}_m^\pm$ in (A.2) to obtain

$$w^{\sigma(\mathbf{s}_m^+)} - w^{\sigma(\mathbf{s}_m^-)} = -k^r + \tau\big(\mathbf{s}_m^+; e^1\mathbf{E}^1, e^r\mathbf{E}^r, e^{r+1}\mathbf{E}^{r+1}\big) - \tau\big(\mathbf{s}_m^-; e^1\mathbf{E}^1, e^r\mathbf{E}^r, e^{r+1}\mathbf{E}^{r+1}\big). \tag{A.6}$$

Let $K \subset S^2$ denote the spherical triangle with vertices $e^1\mathbf{E}^1$, $e^r\mathbf{E}^r$ and $e^{r+1}\mathbf{E}^{r+1}$. If $m \neq m_*$, then neither $\mathbf{s}_m^+$ nor $\mathbf{s}_m^-$ lies in K, so that, by (A.3), both of the τ-terms in (A.6) vanish. On the other hand, if $m = m_*$, then either $\mathbf{s}_{m_*}^+$ or $\mathbf{s}_{m_*}^-$ lies in K but not both, so that one of the τ-terms in (A.6) vanishes while the other is equal to ± 1. Therefore, amongst the four possible values of $w^{\sigma(\mathbf{s}_m^+)} - w^{\sigma(\mathbf{s}_m^-)}$, three will have the same value and one will be different. m_* is identified as the index for which $w^{\sigma(\mathbf{s}_m^+)} - w^{\sigma(\mathbf{s}_m^-)}$ has the different value.

Once the edge signs are determined, the kink numbers can be obtained from (A.6), and hence the trapped area from (A.2).

References

[1] M. Abramowitz, I.A. Stegun, Handbook of Mathematical Functions, Dover Publications, 1965.
[2] G. Birkhoff, Tres observaciones sobre el algebra lineal, Univ. Nac. Tacumán Rev. Ser. A 5 (1946) 147–151.
[3] H. Brezis, The interplay between analysis and topology in some nonlinear PDE problems, Bull. Amer. Math. Soc. 40 (2006) 179–201.
[4] H. Brezis, J.-M. Coron, E.H. Lieb, Harmonic maps with defects, Comm. Math. Phys. 107 (1986) 649–705.
[5] A.J. Davidson, N.J. Mottram, Flexoelectric switching in a bistable nematic device, Phys. Rev. E 65 (2002) 051710.
[6] P.-G. de Gennes, J. Prost, The Physics of Liquid Crystals, second ed., Oxford University Press, 1995.
[7] C. Denniston, J.M. Yeomans, Flexoelectric surface switching of bistable nematic devices, Phys. Rev. Lett. 87 (2001) 275505.
[8] J. Eells, B. Fuglede, Harmonic Maps Between Riemannian Polyhedra, Cambridge Tracts in Mathematics, vol. 142, Cambridge University Press, 2001.
[9] M. Gromov, R. Schoen, Harmonic maps into singular spaces and p-adic superrigidity for lattices in groups of rank one, Publ. IHES 76 (1992) 165–246.
[10] R.M. Hardt, Singularities of harmonic maps, Bull. Amer. Math. Soc. 34 (1997) 15–34.
[11] J.C. Jones, J.R. Hughes, A. Graham, P. Brett, G.P. Bryan-Brown, E.L. Wood, Zenithal bistable devices: Towards the electronic book with a simple LCD, In: Proc IDW, 2000, pp. 301–304.
[12] S. Kitson, A. Geisow, Controllable alignment of nematic liquid crystals around microscopic posts: Stabilization of multiple states, Appl. Phys. Lett. 80 (2002) 3635–3637.
[13] M. Kléman, Points, Lines and Walls, John Wiley and Sons, Chichester, 1983.
[14] M. Kleman, O.D. Lavrentovich, Soft Condensed Matter, Springer, 2002.
[15] O.D. Lavrentovich, Topological defects in dispersed liquid crystals, or words and worlds around liquid crystal drops, Liquid Crystals 24 (1998) 117–125.
[16] F.H. Lin, C.C. Poon, On nematic liquid crystal droplets, in: Elliptic and Parabolic Methods in Geometry, A.K. Peters, 1996, pp. 91–121.
[17] A. Majumdar, Liquid crystals and tangent unit-vector fields in polyhedral geometries, PhD thesis, University of Bristol, 2006.
[18] A. Majumdar, J.M. Robbins, M. Zyskin, Elastic energy of liquid crystals in convex polyhedra, J. Phys. A 37 (2004) L573–L580; J. Phys. A 38 (2005) 7595.
[19] A. Majumdar, J.M. Robbins, M. Zyskin, Lower bound for energies of harmonic tangent unit-vector fields on convex polyhedra, Lett. Math. Phys. 70 (2004) 169–183.
[20] A. Majumdar, J.M. Robbins, M. Zyskin, Elastic energy for reflection-symmetric topologies, J. Phys. A 39 (2006) 2673–2687.
[21] A. Majumdar, J.M. Robbins, M. Zyskin, Topology and bistability in liquid crystal devices, math-ph/0611016, 2006.
[22] N.D. Mermin, The topological theory of defects in ordered media, Rev. Mod. Phys. 51 (C) (1979) 591–651.
[23] C.J.P. Newton, T.P. Spiller, Bistable nematic liquid crystal device modelling, In: Proc. 17th IDRC (SID), 1997, p. 13.
[24] J.M. Robbins, M. Zyskin, Classification of unit-vector fields in convex polyhedra with tangent boundary conditions, J. Phys. A 37 (2004) 10609–10623.
[25] I.W. Stewart, The Static and Dynamic Continuum Theory of Liquid Crystals, Taylor and Francis, London, 2004.
[26] E.G. Virga, Variational Theories for Liquid Crystals, Chapman and Hall, 1994.
[27] G.E. Volovik, O.D. Lavrentovich, Topological dynamics of defects – boojums in nematic drops, Sov. Phys. JETP 58 (1983) 1159.
[28] M. Zyskin, Homotopy classification of director fields on polyhedral domains with tangent and periodic boundary conditions, Preprint, 2005.